Ecological Informatics 82 (2024) 102727

Contents lists available at ScienceDirect

Ecological Informatics

journal homepage: www.elsevier.com/locate/ecolinf

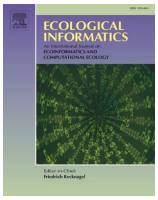

Dynamic evaluation of the ecological evolution and quality of arid and semi-arid deserts in the Aibugai River Basin based on an improved remote sensing ecological index

Haobin Zhang [a], Chao Ma [a,d,e], Pei Liu [b,c,*]

[a] School of Surveying and Land Information Engineering, Henan Polytechnic University, Jiaozuo 454003, China
[b] Hainan Academy of Ocean and Fisheries Sciences, Haikou 572000, China
[c] Yazhou Bay Innovation Institute, Hainan Tropical Ocean University, Sanya 570100, China
[d] Key Laboratory of Spatio-temporal Information and Ecological Restoration of Mines(MNR), Henan Polytechnic University, Jiaozuo 454003, China
[e] Research Centre of Arable Land Protection and Urban-rural High-quality Development in Yellow River Basin, Henan Polytechnic University, Jiaozuo 454003, China

ARTICLE INFO

Keywords:
Ecological quality
Arid and semi-arid regions
New modified remote sensing ecological index
Aibugai River Basin
Sustainable development

ABSTRACT

The ecological quality of arid and semi-arid regions (ASRs) is fragile, and the evaluation of dynamic changes in the multi-factor, long-time-series ecological quality of these regions can provide a scientific basis for sustainable regional development. Based on the remote sensing ecological index (RSEI) and its derivative indices dedicated to monitoring ecological quality in ASRs, this study proposes a new modified RSEI (nmRSEI) suitable for ASRs. We used the nmRSEI to evaluate the dynamic changes in the ecological quality and analyse the factors driving these changes in the Aibugai River Basin in the middle of the Inner Mongolian Plateau in the arid core of Asia from 1986 to 2022. The results led to the following conclusions: (1) the use of the nmRSEI helps solve the problems related to the original greenness index, i.e. normalised difference vegetation index, which was readily affected by the soil background in areas with low vegetation coverage; (2) the new dryness index can meet the evaluation requirements for the surface dryness degree in >98.65% of the study area; (3) the introduced salinity index showed a significant negative correlation with the nmRSEI; (4) the nmRSEI exhibits a gradual downward trend (Slope = −0.00326/10a); and (5) temperature was the main factor controlling the ecological quality during the research period. The nmRSEI provides a fast and effective new method for regularly monitoring ecological quality in ASRs. In addition, driving factor analysis can provide theoretical support for ecological protection in ASRs and the realisation of the United Nations 2030 Sustainable Development Goals.

1. Introduction

Arid and semi-arid regions (ASRs) cover >40% of the land surface and host nearly 40% of the population worldwide and are also among the most sensitive areas susceptible to climate change and anthropogenic activities (Fan et al., 2021; Huang et al., 2019). Owing to climate change, ASRs have expanded since the 20th century (Yin et al., 2019). As a critical part of the global ecosystem, the arid and semi-arid ecosystem responds to global climate change trends (Chen et al., 2018), affects the food security of 14.4% of the worldwide population (Huang et al., 2019), and dominates the annual changes in global carbon sinks (Zhang et al., 2020). Therefore, in the context of global climate change, fast, accurate, and scientific monitoring of the changes in ecological quality in ASRs and understanding their evolutionary patterns are crucial for advancing the realisation of the United Nations Sustainable Development Goals (Zheng et al., 2022).

In recent years, it has been challenging for the ecological quality evaluation methods based on traditional approaches, such as the ecological index (EI)-based approach (Ministry of Ecology and Environment of the People's Republic of China, 2015), to meet the requirements of practical applications because of difficulties in data acquisition accompanied with excessive human intervention (Wen et al., 2022). Owing to the unique advantages of remote-sensing technology, its application in ecological quality monitoring has gradually increased. Hitherto, ecological quality evaluation approaches based on remote sensing can be divided into two main categories, i.e., methods using single-index evaluation and those based on comprehensive indices (Qin et al., 2024). The single-index method primarily employs indicators,

* Corresponding author at: Hainan Academy of Ocean and Fisheries Sciences, Haikou 572000, China.
E-mail addresses: 212104010019@home.hpu.edu.cn (H. Zhang), mac@hpu.edu.cn (C. Ma), cumtlp@gmail.com (P. Liu).

https://doi.org/10.1016/j.ecoinf.2024.102727
Received 21 February 2024; Received in revised form 11 July 2024; Accepted 13 July 2024
Available online 15 July 2024

such as the vegetation index and surface temperature, to evaluate the ecological quality of forests, grasslands, and cities (Liu et al., 2022a; Wang et al., 2021a; Yu et al., 2022a). A single-indicator model can reflect the impact of a particular aspect on ecological quality, but changes in ecological quality are invariably the result of the joint action of multiple factors; therefore, a single indicator can readily lead to unilateral outcomes. The remote sensing ecological index (RSEI), proposed by Xu Hanqiu (Xu, 2013), exhibits strong objectivity and is coupled with four indicators such as greenness, humidity, heat, and dryness represented by normalised difference vegetation index (NDVI), wet component of the tasseled cap transform (WET), land surface temperature (LST) and normalised difference bare soil index (NDBSI), respectively. The RSEI-based model has been extensively tested for urban ecological quality evaluation, e.g., in Fuzhou (Geng et al., 2022), Tianjin (Zhang et al., 2021), and Qingdao (Yang and Li, 2023) cities. Cai et al. (2023) evaluated the ecological quality of wetland ecosystems in the Yellow River Delta using a combination of the RSEI and geoprobes. Chen et al. (2022) assessed the ecological quality changes in the Greater Khingan Mountains using RSEI and identified the significant factors affecting ecological quality. A few researchers have also attempted to apply the RSEI to the evaluation of ecological quality in arid regions, such as in Turpan and Hami cities from 2000 to 2018 (Wang et al., 2022a) and in the Alar reclamation area (Dai et al., 2022). However, the RSEI is designed to evaluate urban ecological quality, and whether the RSEI-based model applies to arid regions remains unclear. Studies have also shown that the results of the RSEI-based evaluation are relatively less stable for areas with extreme ecological conditions (e.g., areas prone to desertification and land degradation) (Zheng et al., 2022). In addition, the ecological indicators selected by the RSEI do not consider the common soil salinisation phenomenon in arid and semi-arid areas and the impact of soil background on the extraction of greenness indicators where vegetation coverage is low. Therefore, the accuracy of the results of the ecological quality analysis is not convincing when the RSEI-based model is directly applied to ASRs.

Recently, a few modified RSEI-based models have been proposed to adapt to the ecological research on ASRs. For example, a modified RSEI (mRSEI)-based model was constructed based on the RSEI and applied to the ecological evaluation in the Qaidam Basin (Jia et al., 2021). This unique difference between the RSEI and mRSEI-based models is that the RSEI adopts the first principal component (PC1) of the principal component analysis (PCA), whereas the mRSEI is composed of the first three components (PC1, PC2, and PC3) of PCA. Although it seems that the mRSEI contains relatively more information, this view is based on an incorrect understanding of the principle of PCA (Xu et al., 2022a). The simple addition of PC2 and PC3 without apparent ecological significance to PC1 with ecological significance leads to the distortion of PC1 and ultimately to a false high evaluation of the ecological quality. In addition, the indicators selected in the mRSEI do not consider the actual situation of an arid area and the soil salinisation phenomenon (Cao et al., 2023); therefore, the mRSEI cannot accurately evaluate the ecological quality of an arid region.

Furthermore, an arid RSEI (ARSEI) was developed based on the RSEI. In this ARSEI-based model, the original dryness of the RSEI was replaced with the salinity index (SI-T), and the soil degradation index was added. Finally, the ARSEI was coupled using greenness, humidity, salinity, heat, and the soil degradation index (Wang et al., 2021b). It is undeniable that the ARSEI-based model considers the general soil salinisation problem in ASRs, but it lacks a dryness index that characterises the degree of surface dryness, which can directly reflect the surface drought in the study area (Xu, 2013; Yang et al., 2023). Similarly, a model called the drought RSEI (DRSEI)-based model was proposed, which introduces the desertification index (DI) and soil-adjusted vegetation index (SAVI) to the RSEI-based model for research in ASRs (Luo et al., 2023). The DRSEI-based model attempts to solve the problem of the impact of the soil background when extracting NDVI in areas with low vegetation coverage. However, the limitation of this model is that the value of the soil adjustment parameter L for SAVI is estimated using empirical data. Although the empirical value of L is 0.5, this parameter has been proven to vary under different vegetation coverages (Liu et al., 2024), and introducing this index to extract the greenness index results in specific errors. The modified SAVI (MSAVI) proposed by Qi et al. (1994) uses a self-adjusting function to replace the soil adjustment parameter L in the original SAVI, which eliminates the impact of the soil background and avoids errors caused by the artificial setting of L.

Current problems encountered in monitoring changes in ecological quality in ASRs using RSEI and its derived indices are as follows:(1) the construction of a few improved RSEI-based models is unreasonable and does not have clear ecological significance; (2) failure to effectively solve the problem of extracting the greenness index in ASRs is affected by the soil background; (3) the original dryness index, i.e. NDBSI, is not applicable in areas with relatively less artificial land cover; (4) and failure to consider soil salinisation effectively, which is highly likely to occur in ASRs.

To meet the demand for evaluating the ecological quality of ASRs, in this study, we coupled five indicators, namely new greenness, humidity, heat, new dryness, and salinity indicators, and proposed a new modified RSEI (nmRSEI). The benefits of the novel approach adopted in this study are as follows: (1) the newly introduced greenness indicator exhibits a higher vegetation signal to soil noise (S/N) ratio than that of the original greenness indicator, i.e. NDVI, and does not require artificial parameterisation, making it relatively more objective; (2) the newly introduced dryness indicator reflects the degradation of the regional surface owing to drying relatively more accurately; and (3) the newly introduced salinity indicator can accurately reflect the regional ecological stress caused by soil salinisation. In this study, we selected the Aibugai River Basin in the Inner Mongolian Plateau, located in the arid and semi-arid climate core region of Eurasia, as the study area, and utilised the nmRSEI to dynamically monitor the ecological quality of the region over a period of 37 years (1986–2022). We analysed the change trends and driving factors of ecological quality and comprehensively verified the rationality, applicability, and superiority of the nmRSEI. The results obtained in this study provide theoretical support for promoting ecological management and sustainable regional development in the ASR.

2. Study area and data selected

2.1. Study area

The Aibugai River is located in the centre of the Inner Mongolian Plateau in the arid core area of Asia. It originates from the Yinshan Mountains southwest of Darhan Maoming'an United Banner (called Damao Banner) in Baotou City. It runs through Darhan Maoming'an United Banner from south to north. The total length is approximately 205 km, the area of the Aibugai River Basin is approximately 0.84×10^4 km^2, and the basin range is located at 109°45′ to 111°02′ east longitude and 41°05′ to 42°31′ north latitude. The terrain of the basin is higher in the south and lower in the north, with low mountains and hills of the Yinshan Mountains in the south (Han et al., 2020) (Fig. 1). The Aibugai River Basin has a temperate continental climate characteristic of ASRs with dry and sandy springs, short and cool summers, and long and cold autumns and winters. The temperature difference between day and night is large in this area, and precipitation is low. The average annual precipitation is approximately 260 mm, mostly concentrated between July and September. The annual evaporation is approximately 2500 mm, much greater than the annual precipitation. The vegetation cover is dominated by desert grasslands, with cultivated land scattered upstream to the south of the basin. The central region, which exhibits the remarkable characteristics of arid desert grasslands in the north, is dominated by desertified grasslands and lacks water resources. Downstream areas in the north are deserted grasslands and bare ground. Thus, the ecological quality of the region is not optimistic (Li et al., 2020; Li et al., 2021; Song et al., 2017).

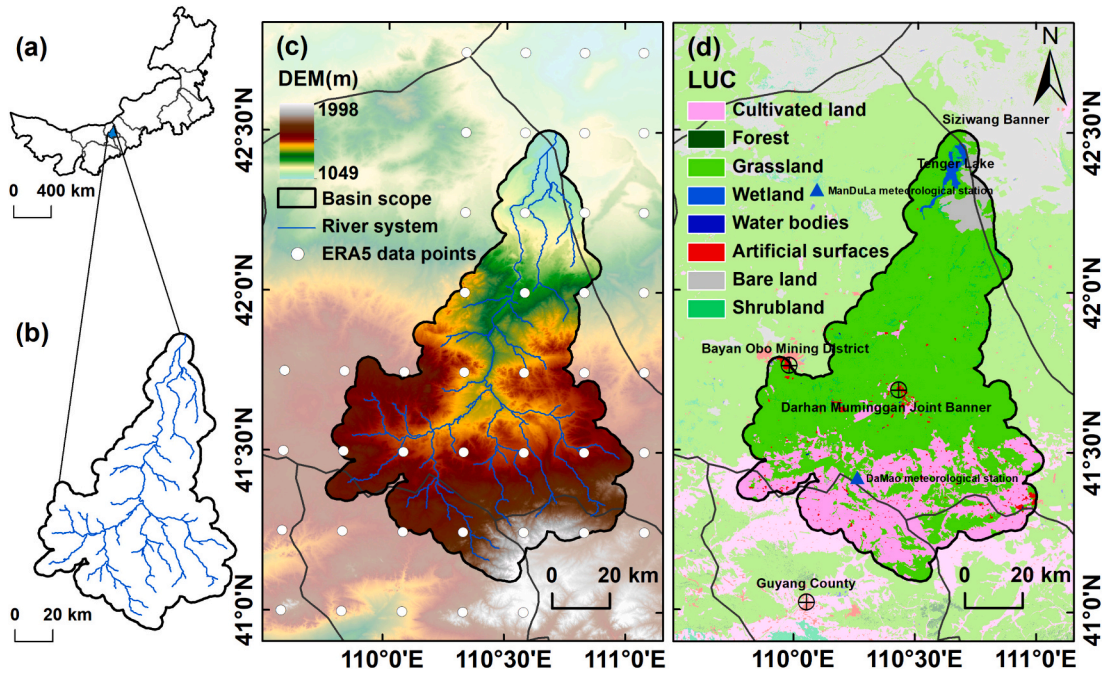

Fig. 1. (a) Geographical location of the study area, and (b) study area and its water system. (c) Topography of the Aibugai River Basin, and (d) land cover types in the Aibugai River Basin.

2.2. Dataset and preprocessing

2.2.1. Landsat satellite images

The selected Landsat thematic mapper (TM) and operational land imager data were obtained from the Geospatial Data Cloud (https://www.gscloud.cn/) and the United States Geological Survey (USGS) (https://earthexplorer.usgs.gov). Ten scenes of remote sensing images were obtained for the July to September period from 1986 to 2022 at 4-years intervals. Precipitation in the study area is mainly concentrated between July and September, and vegetation growth is vigorous during this period. The average cloud cover proportion in the data was maintained at <10% to avoid the impact of clouds (Table 1).

2.2.2. Elevation data

The Shuttle Radar Topography Mission 90-m Digital Elevation Model (DEM) provided by the Consultative Group on International Agriculture Research-Consortium for Spatial Information (CGIAR-CSI) (Jarvis et al., 2008) (https://cgiarcsi.community/) was selected. With the help of the watershed analyses using the DEM, the river network of the Aibugai River was obtained, and the watershed range and vector boundaries were determined.

Table 1
Information regarding remote sensing images.

Year	Strip number	Frame number	Image data	Sensor type	Cloud cover (%)
1986	127	31	1986-08-02	Landsat5-TM	3
1990	127	31	1990-08-13	Landsat5-TM	0
1994	127	31	1994-08-24	Landsat5-TM	0
1998	127	31	1998-07-02	Landsat5-TM	0
2002	127	31	2002-08-30	Landsat5-TM	0
2006	127	31	2006-09-10	Landsat5-TM	0
2010	127	31	2010-09-05	Landsat5-TM	1
2014	127	31	2014-07-30	Landsat8-OLI	0
2018	127	31	2018-07-09	Landsat8-OLI	7.67
2022	127	31	2022-08-05	Landsat8-OLI	0.06

2.2.3. ERA5 meteorological dataset (Hersbach et al., 2020)

There are few meteorological stations in the Aibugai River Basin; therefore, ERA5 was used to reanalyse the meteorological dataset. The ERA-5 dataset is a fifth-generation meteorological dataset (https://cds.climate.copernicus.eu/) released by the European Centre for Medium-Range Weather Forecasts, with a spatial resolution of 0.25° × 0.25° and a time-resolved of 1 h (Li et al., 2022; Xu et al., 2022). It is widely used in hydrological simulations, precipitation prediction, surface air temperature inversion, and other studies (Tang et al., 2022; Xu, 2021; Zhu et al., 2021). The hourly ERA-5 precipitation and temperature data for the Aibugai River Basin from 1986 to 2018 contained 56 grid data centre points (Fig. 1c).

2.2.4. Land cover type dataset

Land cover data were obtained from the global land cover data provided by GlobeLand30 (Jun et al., 2014) (www.globallandcover.com), with a spatial resolution of 30 m × 30 m. Land cover data for 2000, 2010, and 2020 were obtained, and the land cover types were divided into the following three major categories: bare land concentration area (BLCA), grassland concentration area (GLCA), and cultivated land concentration area (CLCA).

2.2.5. Humanities dataset

The dataset describing the total population and the number of sheep and large livestock in Damao Banner, Baotou City, Inner Mongolia, was acquired from the Statistical Yearbooks and Statistical Bulletins for the period from 1986 to 2018 (http://www.dmlhq.gov.cn).

2.2.6. Net primary productivity (NPP) data

These data were obtained from the MOD17A3HGFv061 NPP dataset provided by NASA's Earth Science Data System (https://search.earth

data.nasa.gov/)(Running and Zhao, 2021). The spatial resolution of the data is 500 m × 500 m. As the data was collected since 2000, we obtained NPP data from 2002 to 2022 to evaluate the performance difference between the RSEI- and nmRSEI-based models. Owing to their different spatial resolutions, the NPP data were resampled to a spatial resolution of 30 m × 30 m using bilinear interpolation. In addition, as both RSEI and the nmRSEI are dimensionless, it is necessary to normalise the NPP data to make them relatively more comparable.

3. Methods

The research methodology consisted of four modules: (1) data preparation and preprocessing, which included image registration, radiometric calibration, and atmospheric correction and cropping; (2) model construction, wherein each ecological factor was obtained, normalised, and subjected to band fusion; subsequently, the ecological model was obtained using PCA; (3) change in trend analysis in the time series, mainly including mean trend analysis and Theil–Sen (T–S) median trend analysis combined with Mann–Kendall (M–K) trend analysis; and (4) driver factor analysis. The precipitation and temperature data of the ERA-5 dataset were interpolated using the thin-plate smoothing spline interpolation method, and then a Pearson correlation analysis was performed for precipitation, temperature, and the nmRSEI. A detailed technical flowchart of the study design is presented in Fig. 2.

3.1. Construction of RSEI-based model

(1) RSEI-based mathematical model

The RSEI-based model couples four indicators, i.e., greenness, humidity, and heat and dryness indicators, to comprehensively characterise the ecological quality. The greenness indicator is characterised by NDVI, which reflects the growth status and vegetation coverage. The humidity component of the Kautlr–Thomas Transformation (Crist, 1985) is selected to represent the humidity indicator (WET), which reflects the moisture contained in the corresponding ground object. The heat indicator is represented by LST, which can be obtained by the inversion of the corrected brightness temperature and reflects the surface heat distribution. The dryness indicator is represented by NDBSI, which reflects the degree of surface desertification. Hence, the RSEI-based mathematical model can be described using Eq. (1) (Xu, 2013) as follows:

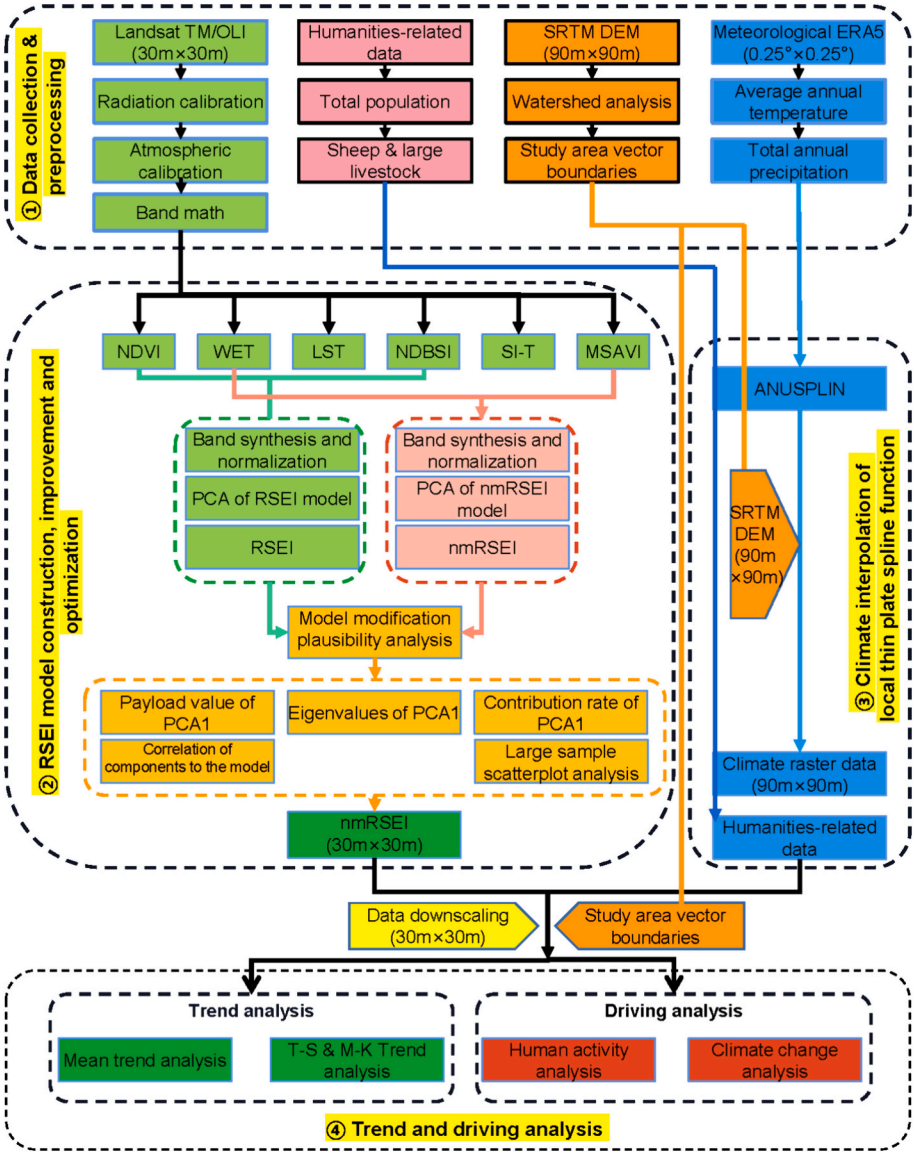

Fig. 2. Technical flowchart of the study design.

$$\mathrm{RSEI} = f\{\mathrm{NDVI}, \mathrm{WET}, \mathrm{LST}, \mathrm{NDBSI}\} \quad (1)$$

(2) nmRSEI-based mathematical model

The proposed nmRSEI-based model introduces MSAVI to solve the problem of the interference of the soil background in the extraction of greenness indicators, using SI-T to characterise the surface soil salinisation phenomenon. Replacing NDBSI with the bare soil index (SI) to characterise surface dryness solves the problem of the non-applicability of the original dryness index NDBSI in ASRs. The nmRSEI-based mathematical model can be described using Eq. (2) as follows:

$$\mathrm{nmRSEI} = f\{\mathrm{MSAVI}, \mathrm{WET}, \mathrm{LST}, \mathrm{SI}, \mathrm{SI} - \mathrm{T}\} \quad (2)$$

In addition, to verify the rationality of replacing the original dryness index NDBSI with the SI, the intelligent building index (IBI) and NDBSI were calculated, and a comparative analysis was performed with the SI. The mixed pixel decomposition method was used to calculate the vegetation coverage fraction (FVC) to quantify the degree of surface vegetation coverage and determine the rationality of replacing NDVI with MSAVI. The calculation methods for each indicator are presented in Table 2.

Table 2
Calculation methods for ecological indicators.

Indicators	Calculation methods
NDVI (Goward et al., 2002)	$\mathrm{NDVI} = \frac{\rho_{nir} - \rho_{red}}{\rho_{nir} + \rho_{red}}$
MSAVI (Lu et al., 2020)	$\mathrm{MSAVI} = \frac{(2\rho_{nir}+1) - \sqrt{(2\rho_{nir}+1)^2 - 8(\rho_{nir} - \rho_{red})}}{2}$
WET (Chen et al., 2019)	$\mathrm{WET_{TM}} = 0.0315\rho_{blue} + 0.2021\rho_{green} + 0.3102\rho_{red} + 0.1594\rho_{nir} - 0.6806\rho_{swir1} - 0.6109\rho_{swir2}$ $\mathrm{WET_{OLI}} = 0.1511\rho_{blue} + 0.1973\rho_{green} + 0.3283\rho_{red} + 0.3407\rho_{nir} - 0.7117\rho_{swir1} - 0.4559\rho_{swir2}$
LST (Chander et al., 2009)	$\mathrm{T} = \frac{K_2}{ln\left(\frac{K_1}{L}+1\right)}$ $\mathrm{LST} = \frac{\mathrm{T}}{\left[1 + \left(\frac{\lambda \mathrm{T}}{\rho}\right)\cdot ln\varepsilon\right]} - 273$
SI (Wang et al., 2021a)	$\mathrm{SI} = \frac{(\rho_{swir1} + \rho_{red}) - (\rho_{nir} + \rho_{blue})}{(\rho_{swir1} + \rho_{red}) + (\rho_{nir} + \rho_{blue})}$
IBI (Xu, 2013).	$\mathrm{IBI} = \frac{\left\{\frac{2\rho_{swir1}}{(\rho_{swir1}+\rho_{nir})} - \left[\frac{\rho_{nir}}{(\rho_{nir}+\rho_{red})} + \frac{\rho_{green}}{(\rho_{green}+\rho_{swir1})}\right]\right\}}{\left\{\frac{2\rho_{swir1}}{(\rho_{swir1}+\rho_{nir})} + \left[\frac{\rho_{nir}}{(\rho_{nir}+\rho_{red})} + \frac{\rho_{green}}{(\rho_{green}+\rho_{swir1})}\right]\right\}}$
NDBSI (Xu, 2013).	$\mathrm{NDBSI} = \frac{SI + IBI}{2}$
SI-T (Pan, 2020)	$\mathrm{SI} - \mathrm{T} = \frac{\rho_{red}}{\rho_{nir}}$
FVC(Liu et al., 2022b)	$\mathrm{FVC} = \frac{(NDVI - NDVI_{soil})}{(NDVI_{veg} - NDVI_{soil})}$

Notes: ρ_{red},ρ_{green} and ρ_{blue} represent the surface reflectance of visible light in the red, green and blue bands, respectively; ρ_{nir} represents surface reflectivity in the near-infrared band; ρ_{swir1} and ρ_{swir2} represent the surface reflectance of shortwave infrared 1 and 2 bands, respectively; T represents the brightness temperature converted from the intensity of thermal radiation, λ is the central wavelength of the thermal infrared band ($\lambda_{TM} = 11.435\ \mu m$, $\lambda_{OLI} = 10.9\ \mu m$) and ρ is a constant value ($\rho = 1.438 \times 10^{-2}\ mK$); ε is the surface emissivity, K_1 and K_2 represent the heat transfer constants (in Landsat 5 TM band 6, $K_1 = 607.76$ $\mathrm{W{\cdot}m^{-2}{\cdot}sr^{-1}{\cdot}\mu m^{-1}}$,$K_2 = 1260.56$ K; in Landsat 8 TIRS band 10, $K_1 = 774.8853$ $\mathrm{W{\cdot}m^{-2}{\cdot}sr^{-1}{\cdot}\mu m^{-1}}$, $K_2 = 1321.0789$ K), and the reflectance after radiation calibration in the thermal infrared band is represented by L. $NDVI_{soil}$ represents normalised difference vegetation index (NDVI) value of pure bare soil; $NDVI_{veg}$ represents NDVI value of pure bare vegetation.

(3) Normalisation of indices

The indicators for constructing the RSEI- and nmRSEI-based models were normalised to make them uniformly dimensionless and to avoid weight imbalance in PCA (Xu, 2013). The normalisation model can be described using Eq. (3) as follows:

$$\mathrm{NI} = \frac{(I - I_{min})}{(I_{max} - I_{min})} \quad (3)$$

where NI is the normalised value of each indicator, the variable I represents the pixel value of the corresponding indicator, I_{min} indicates the minimum value of the indicator, and I_{max} indicates the maximum value of the indicator.

(4) Principal component analysis and result classification

The band synthesis and PCA of normalised indicators were performed. When the payload of indicators positively correlating with ecological quality in the PC1 feature vector is negative or the payload of indicators negatively correlating with ecological quality is positive, it indicates that PC1 is opposite to the ecological status. When this is the case, 1-PC1 is required to obtain the $\mathrm{RSEI_0}$ and $\mathrm{nmRSEI_0}$ (Xu and Deng, 2022). Otherwise, a 1-PC1 calculation is not needed. To facilitate the division of ecological grades, the $\mathrm{RSEI_0}$ must be normalised such that the value of ecological quality is between 0 and 1. For a better understanding, ecological indicators were divided into five levels with an interval length of 0.2 (Xu, 2013), i.e., poor (0, 0.2], fair (0.2, 0.4], moderate (0.4, 0.6], good (0.6, 0.8] and excellent (0.8, 1.0].

3.2. Ratio of vegetation signal to soil noise

When Qi et al. (1994) proposed MSAVI, they introduced a statistical indicator, the S/N ratio, to evaluate the ability of each vegetation index to weaken the impact of soil background. In this study, the S/N ratios of NDVI and MSAVI were calculated to determine the impact of soil background on the extraction of the greenness index. The calculation can be described using Eq. (4) as follows:

$$\mathrm{S/N} = \frac{\overline{VI}}{2\delta}, \quad (4)$$

where $\overline{VI}$ is the mean value of the vegetation index, and δ is the standard deviation of the vegetation index under different vegetation covers. A high S/N ratio indicates that the vegetation index can effectively weaken the impact of soil background.

3.3. Local thin plate smoothing spline interpolation method

Using Python, the annual mean temperature and total annual precipitation values of each grid centre point of the ERA-5 temperature and precipitation data in the study area were calculated. Meteorological data were interpolated using the local thin plate smoothing spline method, i.e., Australian National University Spline (ANUSPLIN), which introduces topographic covariables. After resampling using bilinear interpolation, meteorological raster data with the same spatial resolution as the Landsat data were obtained. The ANUSPLIN is an extension of the thin-plate smoothing spline. Linear cooperative variables can be introduced based on the independent variables of the ordinary spline function. The model can be described using Eq. (5) as follows:

$$Z_i = f(x_i) + b^T y_i + e_i \ (i = 1, \cdots, N), \quad (5)$$

where z_i is the dependent variable located at point i in space, x_i is the d-dimensional vector of the spline independent variables, f is the smoothing function of x_i, y_i is the p-dimensional independent covariate function, b is the p-dimensional coefficient of y_i and e_i is the random

error. In this study, the projection coordinates X and Y were considered as independent variables, DEM as a covariate, and the annual average temperature and annual precipitation as dependent variables. The smoothing function f and coefficient b in the model can be determined by least-squares estimation using Eq. (6) as follows:

$$\sum_{i=1}^{N}\left(\frac{Z_i - f(x_i) - b^T y_i}{w_i}\right)^2 + \rho J_m(f), \tag{6}$$

where $J_m(f)$ represents the roughness measure function of the function $f(x_i)$ and is defined as m, the meso-partial derivative of the function f; ρ is a positive smooth parameter, usually defined by generalised cross validation (GCV), and it plays a balancing role between data fidelity and surface roughness; GCV can be calculated using 'one point move' method, wherein one sample point is removed in turn, and the remaining sample points are used for surface fitting under certain smooth parameters to obtain the estimated value of the point; subsequently, the variance of the observed value is calculated (Guo et al., 2022; Yu et al., 2022b).

3.4. Theil–Sen median trend analysis and M–K trend test

The T–S median trend analysis is a nonparametric trend calculation method. It exhibits the advantages of high efficiency and strong anti-noise ability and can efficiently represent the variation in unit time. The M–K method is a nonparametric statistical test method that can evaluate the significance of trend changes. Hence, in this study, the changing trend of ecological quality was obtained using the T–S median trend analysis, and its significance was tested using the M–K test (Kang et al., 2020). The calculation process included the following two steps:

(1) Calculation of the T–S median trend (Wang et al., 2022b) using Eq. (7) as follows:

$$\beta = Slope = Median\left(\frac{x_j - x_i}{j - i}\right),\ \forall j > i, \tag{7}$$

where x_i and x_j represent nmRSEI time series data, and $1 < i < j < n$; β is the slope. When $\beta > 0$, it implies that the time series shows an upward trend. On the contrary, when $\beta < 0$, the time series shows a downward trend.

(2) Calculation of the pixel-by-pixel M–K test statistic S using Eqs. (8) and (9) (Li et al., 2019; Liu et al., 2022b) as follows:

$$S = \sum_{i=1}^{n-1}\sum_{j=i+1}^{n} sgn(x_j - x_i) \tag{8}$$

$$sgn(x_j - x_i) = \begin{cases} 1 & x_j - x_i > 0 \\ 0 & x_j - x_i = 0 \\ -1 & x_j - x_i < 0 \end{cases} \tag{9}$$

The length of the time series in this study was $n = 10$, and the statistic S approximately obeyed the standard normal distribution; therefore, the statistic Z was used for the trend test. The calculation of Z can be described using Eqs. (10) and (11) as follows:

$$Z = \begin{cases} \dfrac{S-1}{\sqrt{VAR(S)}} & S > 0 \\ 0 & S = 0 \\ \dfrac{S+1}{\sqrt{VAR(S)}} & S < 0 \end{cases} \tag{10}$$

$$VAR(S) = \frac{n(n-1)(2n+5) - \sum_{i=1}^{m} t_i(t_i-1)(2t_i+5)}{18} \tag{11}$$

where n is the number of the nmRSEI-based data in the time series, m represents the number of nodes (recurring datasets) in the time series, and t_i is the width of the nodes (group i is the number of duplicate data in the group). The significance levels considered in the test were as follows: $\alpha = 0.1$, $Z_{1-\frac{\alpha}{2}} = Z_{0.950} = 1.645$ $\alpha = 0.05$, $Z_{1-\frac{\alpha}{2}} = Z_{0.975} = \pm 1.96$; and $\alpha = 0.01$, $Z_{1-\frac{\alpha}{2}} = Z_{0.995} = \pm 2.58$.

4. Results and analysis

4.1. Rationality analysis of replacing NDBSI and introducing MSAVI

4.1.1. Rationality analysis of SI replacing NDBSI

Based on the characteristics of land cover obtained from GlobeLand30 land use/ cover data in the study area, the construction index IBI was abandoned, and only the SI was reserved to describe the desiccation and degradation of the surface. To verify the feasibility of this modification, the NDBSI, SI and IBI indicators were calculated, and the average values are listed in Table 3.

It can be seen from Table 3 that the mean values of the SI were the largest among the three selected indicators, the mean values of NDBSI were between those of SI and IBI, and the mean values of IBI were the smallest. The initial dryness index, i.e., NDBSI, will lead to an underestimation of the bare land surface and an overestimation of buildings and artificial surface areas. To further support the finding, the 'bare land', 'grassland', 'buildings' and 'cultivated land' in the study area were sampled (Fig. 1d), and the mean values of NDBSI, SI, and IBI were calculated (Fig. 3).

As shown in Fig. 3, the trend of the average values of the three indicators of the four land cover types was SI > NDBSI>IBI. The trend of the average values of the SI for different land cover types was SI_bare land>SI_grassland>SI_cultivated land>SI_building, indicating that the SI can effectively extract surface bareness. The values of IBI in all land cover areas were low (the value range was −0.043 to 0.14), and the land cover data provided by GlobeLand30 showed that the proportion of building land in the study area was approximately 1.35%. Therefore, if 1/2 weight is set for the model construct, NDBSI will underestimate the overall degree of desiccation in the study area, which will inevitably have a crucial impact on the evaluation of dryness. In contrast, the SI can cover 98.65% of the study area, excluding construction land. Hence, constructing a dryness index using the SI can better reflect the ecological degradation in ASRs.

4.1.2. Rationality analysis of MSAVI replacing NDVI

The study area belongs to the ASR, and the land cover types are desert grassland and bare land. It was found through calculations that the average FVC was between 0.253 and 0.438; therefore, the soil background restricted the extraction of greenness indicators.

The S/N ratios of the two vegetation indices were calculated to test the effects of the green indices extracted using MSAVI and NDVI (Table 4).

As shown in Table 4, the S/N ratio calculated using NDVI was between 0.849 and 1.593, and that estimated using MSAVI was between 1.168 and 2.098. Thus, the value of the S/N ratio calculated using MSAVI was greater than that obtained using NDVI for all analysed years. It was preliminarily announced that the replacement of NDVI with MSAVI could effectively reduce the impact of the soil background on the extraction of greenness indicators. To further verify this point of view, the study area was divided into BLCA, GLCA, and CLCA, and the NDVI and MSAVI were calculated. The S/N ratios of all these regions were calculated to determine the interference of the soil background in the extraction of the green index under different land cover types (Fig. 4).

As shown in Fig. 4, the trend of the S/N ratios of different land cover types was as follows: S/N_BLCA MSAVI>S/N_BLCA NDVI, S/N_GLCA MSAVI>S/N_GLCA NDVI and S/N_CLCA MSAVI>S/N_CLCA NDVI. This result further indicates that, compared with NDVI, MSAVI can weaken

Table 3
Annual mean values of normalised difference bare soil index (NDBSI), bare soil index (SI) and intelligent building index (IBI) in each analysed year during the study period.

Indicators	Year									
	1986	1990	1994	1998	2002	2006	2010	2014	2018	2022
Mean NDBSI	0.134	0.093	0.036	0.145	0.121	0.135	0.139	0.097	0.134	0.098
Mean SI	**0.174**	**0.135**	**0.076**	**0.183**	**0.161**	**0.172**	**0.177**	**0.131**	**0.169**	**0.130**
Mean IBI	0.095	0.052	−0.004	0.108	0.080	0.097	0.101	0.063	0.098	0.065

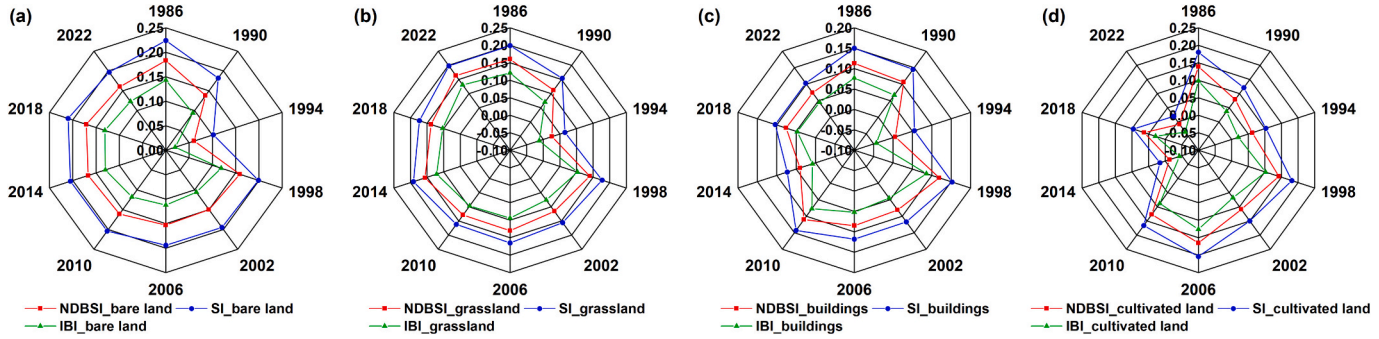

Fig. 3. Annual mean values of sampled normalised difference bare soil index (NDBSI), bare soil index (SI) and intelligent building index (IBI) for each analysed year during the study period.

Table 4
Ratios of vegetation signal-to-soil noise calculated using normalised difference vegetation index (NDVI) and modified soil-adjusted vegetation index (MSAVI).

Vegetation index	Year									
	1986	1990	1994	1998	2002	2006	2010	2014	2018	2022
S/N_NDVI	1.249	1.325	1.585	1.488	1.333	1.593	1.206	0.849	1.065	0.875
S/N_MSAVI	**1.587**	**1.831**	**2.098**	**1.923**	**1.775**	**2.021**	**1.633**	**1.168**	**1.406**	**1.255**

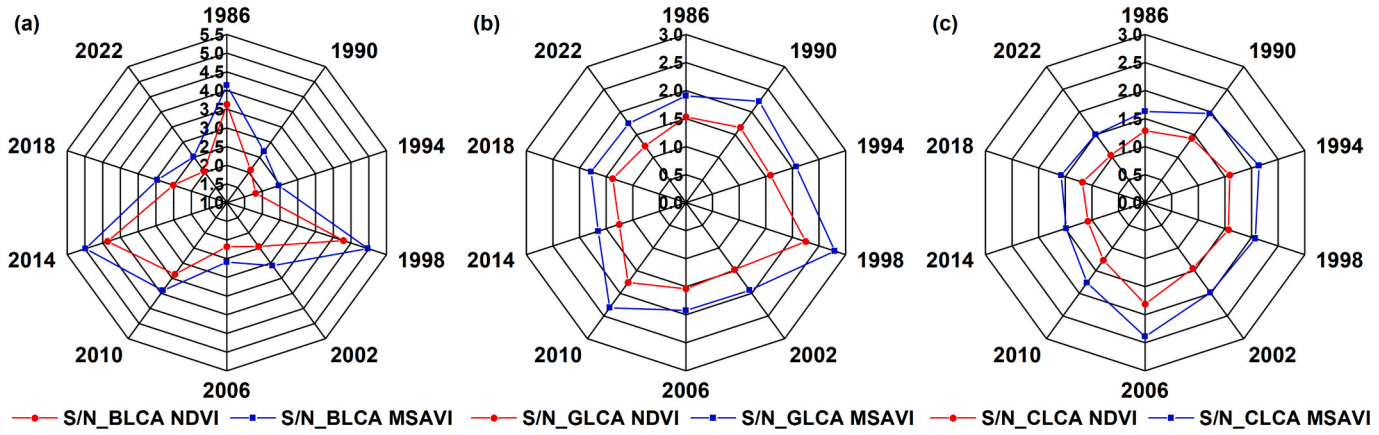

Fig. 4. Vegetation signal-to-soil noise ratios calculated using normalised difference vegetation index (NDVI) and modified soil-adjusted vegetation index (MSAVI) under different land cover types.

the impact of soil background on the extraction of greenness indicators.

The S/N ratios calculated using MSAVI differed significantly under different land cover types (S/N_BLCA MSAVI>S/N_GLCA MSAVI>S/N_CLCA MSAVI). This finding indicating that the ability of MSAVI to weaken the impact of soil background on the extraction of greenness indicators is stronger in areas with low vegetation coverage than in those with abundant vegetation coverage. Therefore, the introduction of MSAVI will render the greenness index relatively more accurate.

4.2. Rationality analysis of the nmRSEI-based model

The effective load of each component of PC1 of the two models, the contribution rate of PC1, and the eigenvalues (EV) can be obtained by performing PCA on the RSEI- and nmRSEI-based models. The payload can reflect whether the impact of the ecological component on the model is positive or negative and can also determine the rationality of the model construction. The contribution rate and EV reflect the ability of the information contained in each ecological factor to test model performance. The rationality and advantages of the nmRSEI were verified by comparing the PCA results of the nmRSEI- and RSEI-based

models.

The payload of each component of PC1 in the RSEI-based model has the following characteristics: components that correlated positively with ecological quality exhibited the same sign, whereas components that correlated negatively with ecological quality exhibited different signs (Xu and Deng, 2022). A comparison of the payload of each PC1 component helped determine the rationality of the model (Table 5).

Table 5 shows the following results:

(1) In the RSEI-based model, the greenness and humidity indicators that correlated positively with ecological quality exhibited similar signs, and the heat and dryness indicators that correlated negatively with ecological quality also showed similar signs. In the constructed nmRSEI-based model, the greenness and humidity indicators that correlated positively with ecological quality in each analysed year exhibited similar signs, as exhibited by the heat, dryness, and salinity indicators that correlated negatively correlated with ecological quality. These results indicate that the nmRSEI meets the requirements of the RSEI construction and that the introduction of the SI-T exerts a negative impact on ecological quality.
(2) Comparing the absolute values of the payloads of the two models, the positive effects of greenness and humidity in the RSEI-based model are slightly greater, and the negative effects of heat and dryness are significantly greater than those in the nmRSEI-based model. In the nmRSEI-based model, the absolute value of the payload of the salinity indicator was greater than the absolute values of the payloads of heat and dryness indicators, indicating that the negative impact of the salinity indicator on ecological quality was relatively more significant.

Based on the principle of PCA, it can be seen that the larger the percentage of the contribution rate of PC1 EV, the greater the amount of information it contains (Xu and Deng, 2022). The model's ability to comprehensively represent ecological components was determined by comparing the contribution rate and EV of PC1 for each model in different years (Table 6).

Table 6 shows the following results: (1) the contribution rate of PC1 of the nmRSEI-based model is 55.48–79.94%, with 69.70% as the average value, greater than that of PC1 of the RSEI-based model; moreover, the contribution rate of PC1 of the nmRSEI-based model was greater than that of the RSEI-based model for 7 of the 10 analysed years, indicating that the nmRSEI-based model better integrated the characteristics of the five ecological factors; (2) the EVs of PC1 for the nmRSEI-based model ranged from 0.01 to 0.058 and were greater than those of the RSEI-based model, indicating that the nmRSEI-based model contained relatively more information than that in the RSEI-based model; and (3) the contribution rate of PC1 in 1986, 2010 and 2018 was relatively low, which can be attributed to the quality of the remotely sensed data, i.e., the higher the proportion of cloud cover, the lower the contribution rate of PC1. Despite the relatively low contribution of PC1 in 1986, 2010, and 2018, Table 5 shows that the PC1 payloads in these 3 years satisfy the requirements for the construction of RSEIs, i.e., ecologically beneficial and unfavourable indices were divided into two distinct groups, suggesting that PC1 has an ecological significance.

4.3. Comparative analysis of the RSEI- and nmRSEI-based models

4.3.1. Correlation analysis between ecological factors and the comprehensive index

Through a correlation analysis between the RSEI- and nmRSEI-based models and various ecological indicators, the inherent relationship between the two models and ecological factors was revealed (Fig. 5) as follows:

(1) The values of correlation coefficients between the RSEI and greenness indicators were smaller than those between the nmRSEI and greenness indicators for all analysed years. The average correlation coefficient value between the RSEI and greenness indicators was 0.662, and that between the nmRSEI and greenness indicators was 0.909. The nmRSEI-based model was relatively more sensitive to changes in the greenness indicators. The average correlation coefficient between the RSEI and humidity index was 0.804, and that between the nmRSEI and humidity index was 0.736, indicating that the humidity index correlated strongly with the RSEI-based model. The likely reason for this result is that the greenness index extracted by MSAVI is relatively more accurate than that extracted by NDVI, leading to a larger weight of MSAVI in PCA, which further weakens the impact of humidity indicators.
(2) The absolute mean values of the correlation coefficients between the RSEI-based model and heat and dryness indicators were

Table 5
Effective payload values of the first principal component (PC1) in remote sensing ecological index (RSEI)- and new modified RSEI (nmRSEI)-based models.

Year	Model	Greenness		Humidity	Heat	Dryness		Salinity
		NDVI	MSAVI	WET	LST	NDBSI	SI	SI-T
1986	RSEI	0.113	/	**0.533**	**−0.803**	**−0.242**	/	/
	nmRSEI	/	**0.410**	0.376	−0.077	/	−0.154	−0.813
1990	RSEI	**0.417**	/	**0.631**	**−0.507**	**−0.414**	/	/
	nmRSEI	/	−0.339	−0.433	0.343	/	0.298	0.701
1994	RSEI	**0.466**	/	**0.514**	**−0.269**	**−0.668**	/	/
	nmRSEI	/	0.333	0.326	−0.150	/	−0.495	−0.718
1998	RSEI	**0.504**	/	**0.616**	**−0.222**	**−0.564**	/	/
	nmRSEI	/	0.390	0.331	−0.164	/	−0.339	−0.772
2002	RSEI	**0.477**	/	**0.570**	**−0.558**	**−0.368**	/	/
	nmRSEI	/	−0.352	−0.409	0.372	/	0.273	0.704
2006	RSEI	**−0.429**	/	**−0.404**	**0.542**	**0.599**	/	/
	nmRSEI	/	−0.374	−0.268	0.256	/	0.379	0.761
2010	RSEI	0.228	/	**0.283**	**−0.874**	−0.323	/	/
	nmRSEI	/	**−0.375**	−0.257	0.342	/	**0.337**	0.750
2014	RSEI	**0.355**	/	**0.222**	**−0.840**	**−0.345**	/	/
	nmRSEI	/	−0.324	−0.187	0.580	/	0.321	0.649
2018	RSEI	0.123	/	**0.279**	**−0.904**	**−0.298**	/	/
	nmRSEI	/	**−0.477**	−0.175	0.419	/	0.296	0.692
2022	RSEI	**0.474**	/	**0.265**	**−0.703**	**−0.460**	/	/
	nmRSEI	/	0.397	0.197	−0.445	/	−0.357	−0.691

Abbreviations: NDVI, normalised difference vegetation index; MSAVI, modified soil-adjusted vegetation index; WET, wet component of the tasseled cap transform; LST, land surface temperature; NDBSI, normalised difference bare soil index; SI, bare soil index; SI-T, salinity index.

Table 6
Comparison of the results of the principal component analysis (PCA) obtained using the remote sensing ecological index (RSEI)- and new modified RSEI (nmRSEI)-based models.

PCA results	Model	1986	1990	1994	1998	2002	2006	2010	2014	2018	2022
PC1 and eigenvalue	RSEI	0.010	0.015	0.015	0.005	0.012	0.007	0.010	0.035	0.008	0.020
	nmRSEI	**0.016**	**0.028**	**0.026**	**0.010**	**0.021**	**0.012**	**0.014**	**0.058**	**0.010**	**0.037**
PC1 contribution rate%	RSEI	**59.20**	73.17	64.41	69.01	72.34	59.78	**63.14**	77.00	**69.16**	74.86
	nmRSEI	55.50	**79.59**	**69.95**	**74.67**	**77.38**	**66.95**	58.36	**79.14**	55.48	**79.94**

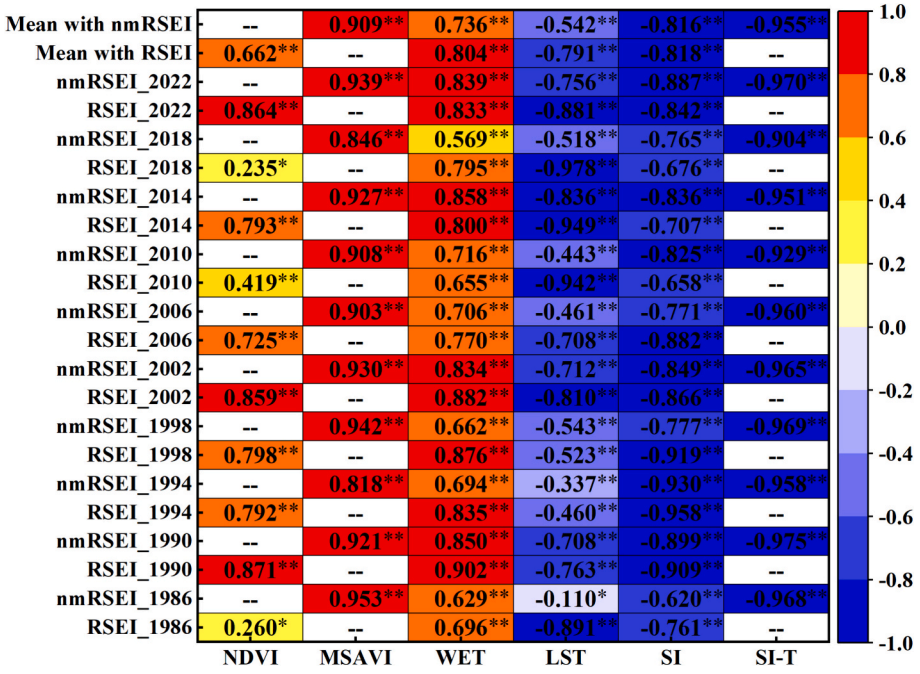

Fig. 5. Correlation between various indicators and remote sensing ecological index (RSEI) and new modified RSEI (nmRSEI).
* indicates significance at $P < 0.05$ and ** indicates high significance at $P < 0.01$.

greater than those between the nmRSEI-based model and these indicators, indicating that heat and dryness indicators exert a greater impact on the RSEI-based model. Moreover, the absolute mean value of the correlation coefficient between SI-T and the nmRSEI-based model is greater than that between heat and dryness indicators and the nmRSEI-based model, indicating that the negative impact of nmRSEI mainly comes from SI-T. Notably, SI-T has a larger weight in PCA than those of heat and dryness indicators, which further indicates that the introduction of SI-T is important for ecological quality assessment in arid and semi-arid areas.

4.3.2. Scatter plot analyses

To further verify the reliability of the nmRSEI-based model, scatter plot analysis was performed for both nmRSEI- and RSEI-based models (Fig. 6). To avoid subjective factors from interfering with the selection of points of interest (POI), a total of 20,000 POI were randomly generated within the study area using the geographic information system package, and the corresponding pixel values of the RSEI and nmRSEI were extracted using POI.

Fig. 6 shows that the correlation between the RSEI and nmRSEI was high, the Pearson correlation coefficient was between 0.472 and 0.969, and these values were all statistically significant, located at the significance level of *P*-value<0.01. The standard deviation of the RSEI and nmRSEI was between 0.03 and 0.092, particularly the data dispersion was relatively large in the years 1986, 2010 and 2018. The coefficient of determination (R^2) of the linear fitting was between 0.223 and 0.940, and the fitting effect was poor in the years 1986, 2010, and 2018. In addition, the RSEI exhibited poor reliability, as there were relatively more discrete points on one side of the RSEI-based model.

The result of the scatter plot analysis of the total pixel values of the two models in 10 years ($n = 200{,}000$) is shown in Fig. 6k. The Pearson correlation coefficient was 0.852, which satisfied the significance test at the level of *P*-value<0.01, indicating that the two models exhibit a significant correlation. From the distribution of scatter clusters, it can be seen that there are relatively more discrete points on the RSEI side, indicating that the RSEI-based model yielded poor stability during the entire study period.

4.3.3. Comparative analysis of the outcomes of the RSEI, nmRSEI, and EI

As it is difficult to verify the accuracy of the results of the comprehensive analysis of ecological quality, in this study, the improvement of the model and the credibility of outputs were verified by a comparative analysis of the average values of the RSEI, nmRSEI, and the introduced third-party data, the EI. As the value of the EI ranges from 0 to 100 and the values of the RSEI and nmRSEI range from 0 to 1, the mean values of the RSEI and nmRSEI need to be multiplied by 100 (Table 7). It must be noted that the environmental quality status bulletin issued by the Department of Ecology and Environment of the Inner Mongolia Autonomous Region provides information regarding the ecological and environmental quality status of the entire autonomous region without specifying the EI. Therefore, the EI value of the Damao Banner region in Table 7 is a range value that corresponds to the ecological evaluation level. Table 7 shows that based on the perspective of model outputs, the values of the nmRSEI were closer to those of the EI between 2006 and 2018. However, based on the perspective of ecological quality levels, the

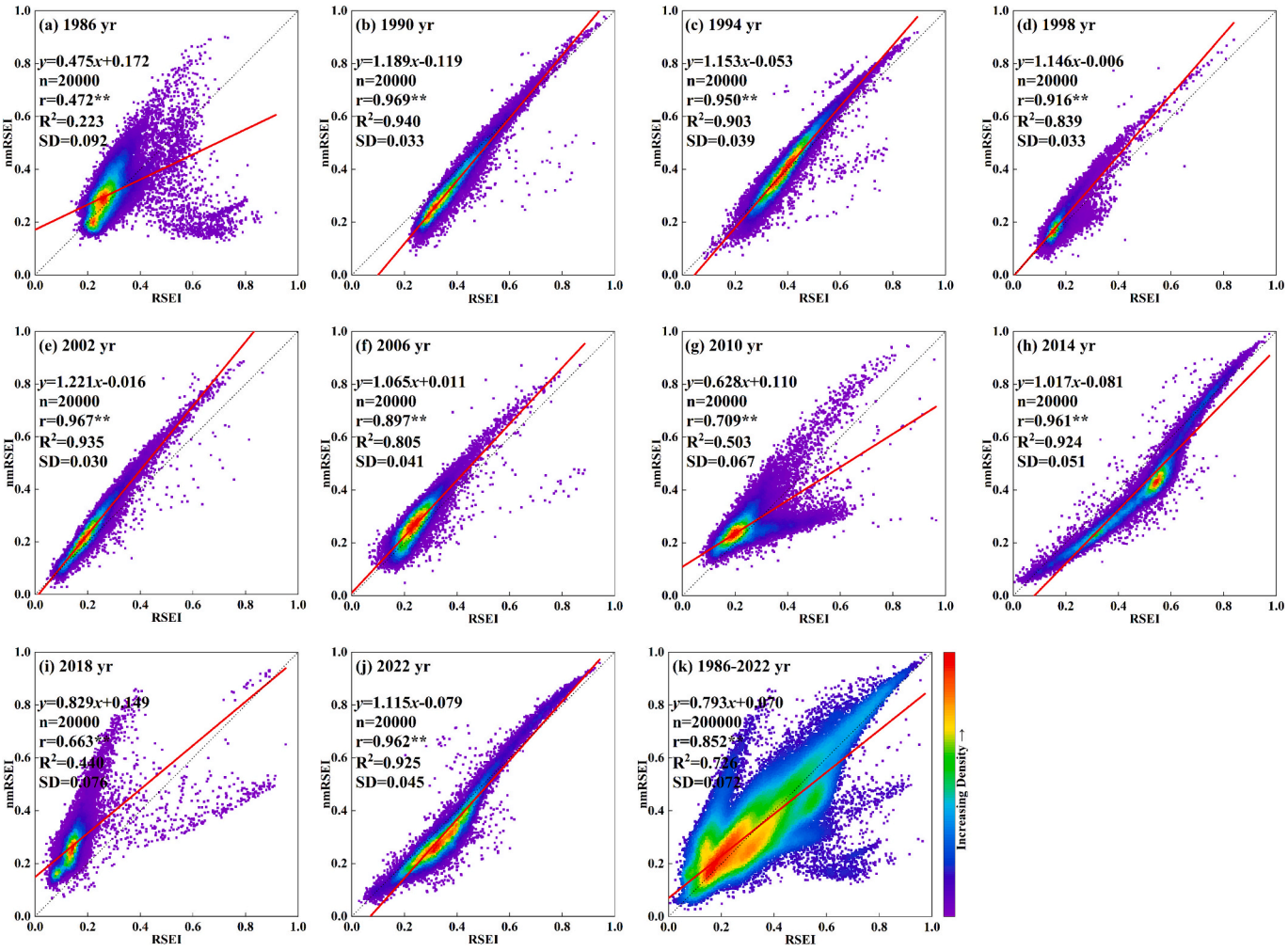

Fig. 6. Scatter plots of the remote sensing ecological index (RSEI) and new modified RSEI (nmRSEI).

Table 7
Comparison of the ecological index (EI), remote sensing ecological index (RSEI), and new modified RSEI (nmRSEI).

Year	2006	2010	2014	2018
Mean RSEI	24.9	26.0	**47.1**	15.0
RSEI level	Fair	Fair	Moderate	Poor
Mean nmRSEI	**27.6**	**27.3**	39.7	**27.3**
nmRSEI level	Fair	Fair	Fair	Fair
EI value	35 ≤ EI<55	35 ≤ EI<55	35 ≤ EI<55	35 ≤ EI<55
EI level	Criticality	Criticality	Criticality	Criticality

Note: The average values of the RSEI and nmRSEI presented in the table were multiplied by 100.

values of EI were relatively stable on average, and those of the nmRSEI were also relatively stable, whereas the values of the RSEI fluctuated greatly. Therefore, it is relatively more reasonable and reliable to use the nmRSEI-based model than the RSEI-based model to perform a comprehensive evaluation of the ecological quality in the study area.

4.4. Dynamic changes in ecological quality assessed using the nmRSEI-based model

4.4.1. Spatial distribution of ecological quality

Time-series spatial distribution maps of ecological quality were obtained based on the nmRSEI results. Fig. 7 shows the following results:

During the study time series, the ecological quality of the study area mainly transformed between 'poor', 'fair' and 'moderate' levels, and there were apparent differences in the ecological quality of different land cover areas. The BLCA covered 297 km^2, and the ecological quality was mainly 'poor' and 'fair', with the percentage range of these two levels being 4.73–98.85% and 1.13–77.34%, respectively. The GLCA covered 4949 km^2, where the ecological quality was 'poor' in 1998 and 'fair' in the other analysed years, and the percentage of the fair ecological quality level was between 18.24 and 83.03%. The CLCA covered 3171 km^2, and the dominating ecological quality was 'fair' and 'moderate', with the percentage range of these two levels being 12.27–84.36% and 5.85–53.77%, respectively. The ecological quality of the CLCA was relatively better compared with that of the GLCA and BLCA. In general, the areas with excellent, fair, and moderate ecological quality levels were mainly located in the 'CLCA' in the southern part of the study area. The ecological quality changed to fair and poor levels as the latitude increased, particularly in the BLCA and GLCA in the northern part, where poor ecological quality was dominant during the study period.

Compared with the ecological quality in 1986, the ecological quality in 1994 improved significantly but deteriorated again in 1998, and the area with poor ecological quality gradually expanded to the southern region. The ecological quality has improved slightly since 2002, but the poor and fair levels of ecological quality continue to dominate. It improved significantly in the southern region in 2014; however, this improvement was not sustainable in the subsequent years because overall, the heat, dryness, and salinity indicators of the study area were higher in 2018, and the overall greenness and humidity indicators were

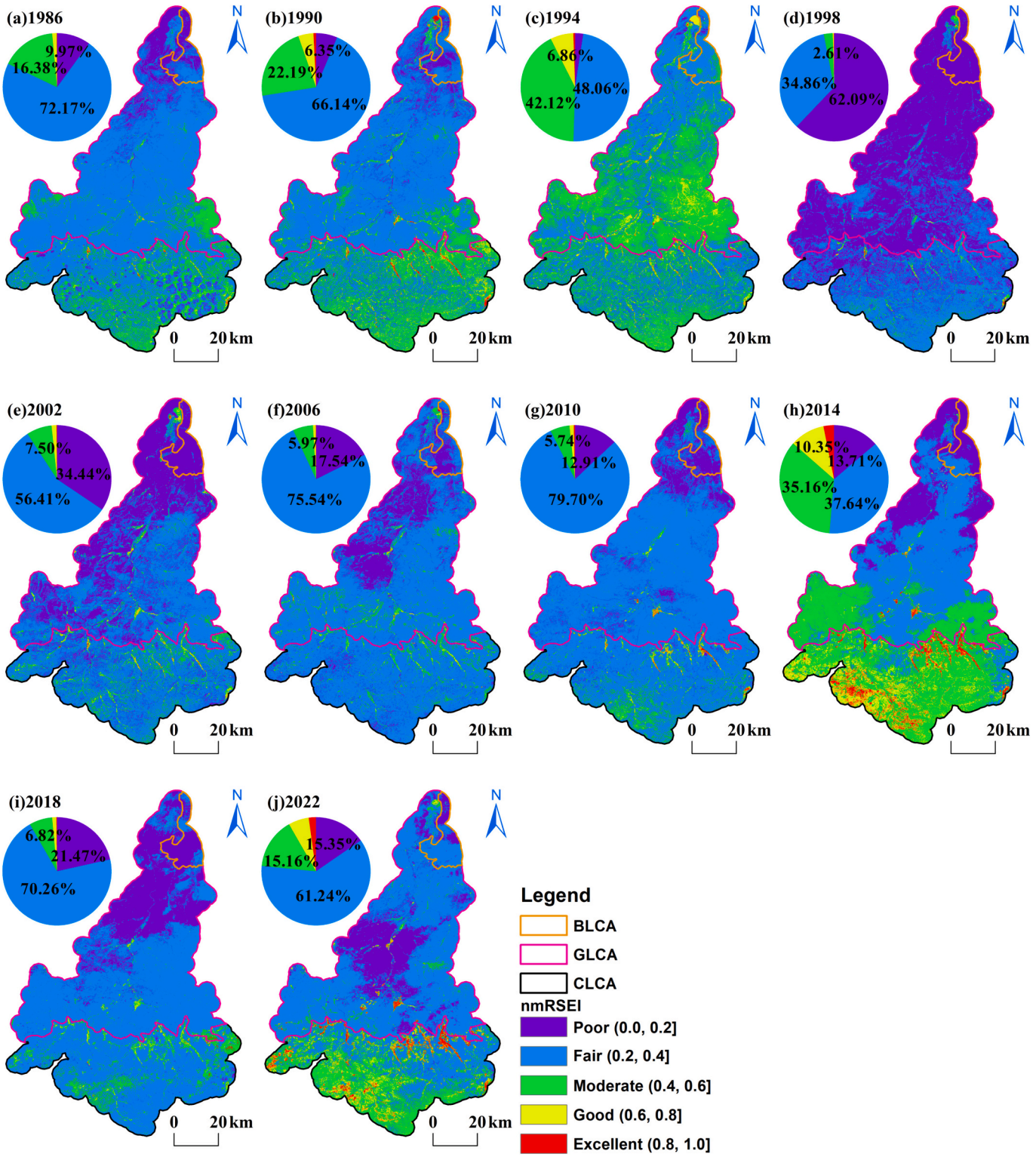

Fig. 7. New modified remote sensing ecological index (nmRSEI)-based distribution maps of the ecological quality levels in the Aibugai River Basin from 1986 to 2022.

lower than that in 2014. Therefore, the ecological quality of the study area in 2018 was worse than in 2014.

4.4.2. Analysis of trends in changes in ecological quality

(1) Trend analysis of the mean changes in ecological quality evaluated using the nmRSEI and the M–K mutation test. To explore the multiyear variation trend evaluated using the nmRSEI, the mean value and trend of the nmRSEI for each analysed year in the study time series were extracted. Fig. 8a shows that the nmRSEI generally exhibited a slightly fluctuating downward trend in the study time series, with a change rate of −0.003 per decade. In addition, the mean value of the nmRSEI changed in stages. From 1986 to 1998, it exhibited a declining trend. A gradual upward

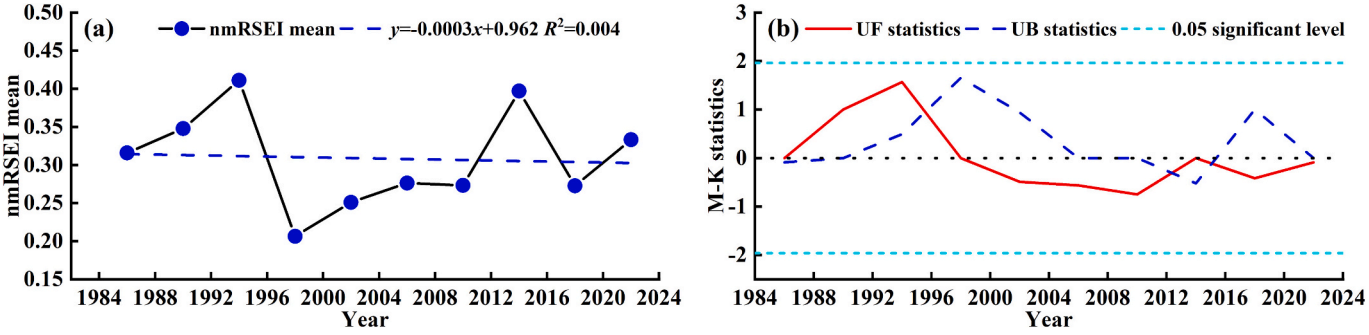

Fig. 8. Changing trends in (a) the mean values of the new modified remote sensing ecological index (nmRSEI) and (b) the Mann–Kendall (M–K) test statistics from 1986 to 2022.

trend was observed between 1998 and 2014, and the period from 2014 to 2022 showed a gradual decline. The periodic changes in the mean value were consistent with the corresponding changes in the nmRSEI-based spatial distribution of ecological quality levels shown in Fig. 7.

The nonparametric M–K test method was used to detect mutations in the mean value of nmRSEI during 1986–2022 and to obtain the mutation nodes of the nmRSEI. The test results are presented in Fig. 8b. There were three points of intersection between the UF and UB curves from 1986 to 2022, i.e., from 1994 to 1998, 2010 to 2014, and 2014 to 2018. However, the variation range of the UF and UB curves after intersection did not exceed the confidence interval, indicating a mutation trend in the nmRSEI during the study time series, but the mutation was not significant.

(2) Trend analysis using the T–S analysis method combined with the M–K approach. To further reveal the trend of changes in ecological quality from 1986 to 2022 in the study area, the T–S method combined with the M–K trend analysis method was used for pixel-by-pixel analysis. The results of this trend analysis were divided into seven levels, i.e., extremely significant decrease, a significant decrease, no significant decrease, no change, no significant increase, a significant increase, or extremely significant increase (Fig. 9). During the study period, the percentage of area with 'degraded' ecological quality degraded was 2.32%, primarily located in the 'GLCA'; the percentage of area with 'no change' in ecological quality was 95.77%, distributed throughout the study area, indicating that the overall ecological quality of the study area was relatively stable; and the percentage of area with 'improved' ecological quality was 1.91%, mostly placed in the 'CLCA', indicating that anthropogenic activities exert a certain promotion effect on the ecological quality. Overall, the percentage of area with 'degraded' ecological quality in the Aibugai River Basin from 1986 to 2022 was 0.41% higher than that of the area with 'improved' ecological quality, indicating that the ecological quality of the Aibugai River exhibited a slight decline during the study period.

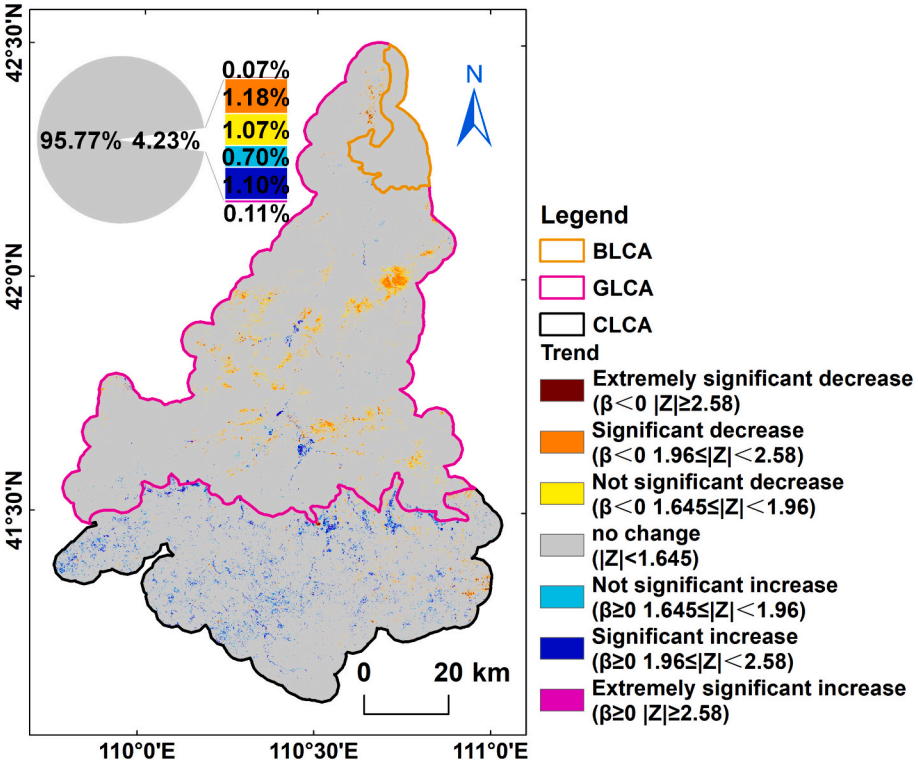

Fig. 9. Spatial distribution of ecological changes in the Aibugai River Basin from 1986 to 2022.

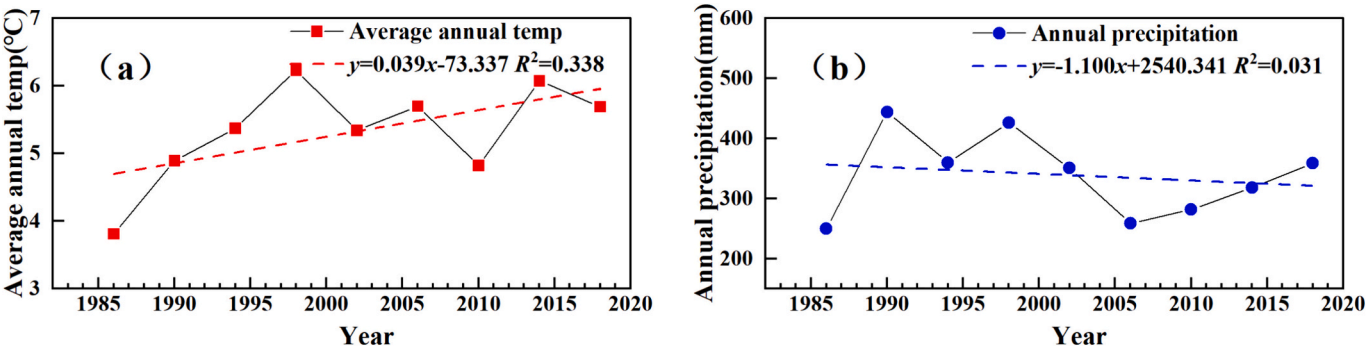

Fig. 10. Changing trends in annual average temperature (a) and total precipitation (b) in the study area.

4.5. Analysis of driving factors

4.5.1. Trends in climate change

The obtained annual average temperature and precipitation maps (Fig. 10) for the 1986 to 2018 period reveal the following results:

(1) the temperature in the study area showed a fluctuating rising trend with a change rate of 0.39 °C per decade. In detail, the temperature increased rapidly from 1986 to 1998, with a change rate of 1.94 °C per decade; subsequently, it showed a downward trend from 1998 to 2010, with a change rate of −0.97 °C per decade. However, from 2010 to 2018, the temperature again showed an upward trend, with a change rate of 1.09 °C per decade. Although the rate of increase in temperature slowed at the beginning of the 21st century, it continued to show an upward trend.

(2) The annual precipitation in the study area showed an overall downward trend, with a change rate of −11 mm per decade. Initially, the precipitation showed an upward trend, with a change rate of −110.97 mm per decade from 1986 to 1998. However, from 1998 to 2006, it exhibited a downward trend, with a change rate of −209.26 mm per decade. From 2006 to 2018, the precipitation again showed an upward trend, and the rate of change was 84.40 mm per decade. In general, although the precipitation has been increasing since the beginning of the 21st century, the overall precipitation during the study period showed a downward trend owing to the rapid decline in precipitation from 1998 to 2006.

4.5.2. Correlation analysis of climate and ecological indicators

A correlation analysis between the mean nmRSEI and annual temperature and precipitation values for the 1986 to 2018 period was performed. The results showed that the Pearson correlation coefficient between the mean nmRSEI and mean annual temperature was 0.145 (P-value = 0.710 > 0.05), and that between the mean nmRSEI and mean annual precipitation was 0.052 (P-value = 0.895 > 0.05). It needs to be noted that the correlation coefficients obtained using the mean value of the nmRSEI did not pass the significance test, and the results acquired using the mean value were not reliable. Therefore, a pixel-to-pixel correlation analysis between the nmRSEI and meteorological data was performed in this study.

(1) Correlation analysis year-by-year

Fig. 11 shows the map depicting the changes in correlation coefficient values (Fig. 11) estimated using the correlation analysis of the nmRSEI data with the precipitation and air temperature data for each analysed year. As shown in Fig. 11 the nmRSEI correlated positively with precipitation, and the correlation coefficient value was between 0.244 and 0.567, with the average value being 0.431. However, it correlated negatively with temperature, and the correlation coefficient value was between −0.184 and − 0.752, with the average value being −0.473. The absolute values of the correlation coefficients between the nmRSEI and precipitation and temperature showed a downward trend from 1986 to 1994 and 1998 to 2006 but an upward trend from 2010 to 2018. The results revealed periodic fluctuations in the correlation between the nmRSEI, precipitation, and temperature.

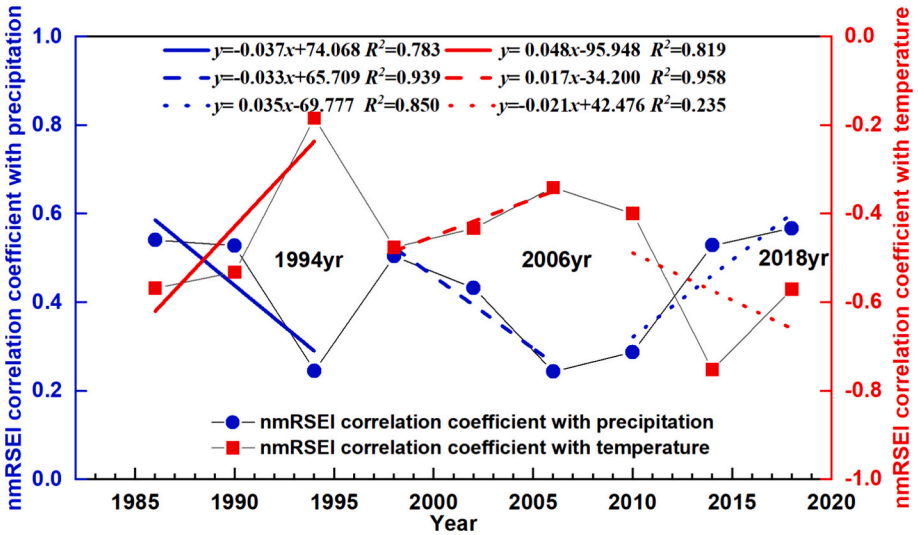

Fig. 11. Temporal changes in the correlation coefficients between the new modified remote sensing ecological index (nmRSEI) and meteorological factors.

(2) Time series correlation analysis

We further explored the spatial diversity of the impact of temperature and precipitation on ecological quality. The nmRSEI data from 1986 to 2018 were used as the test dataset in the pixel-by-pixel correlation analysis and significance tests conducted with the corresponding annual average temperature and annual precipitation datasets (Fig. 12). The correlation results were divided into four categories, i.e. significant positive correlation (P-value<0.05, $r > 0$), no significant positive correlation (P-value≥ 0.05, $r > 0$), significant negative correlation (P-value<0.05, $r < 0$) and no significant negative correlation (P-value≥ 0.05, $r < 0$).

It can be seen that the percentage of the areas where the nmRSEI correlated negatively with temperature was 73.96%, mainly located in the 'GLCA' and 'BLCA'. The percentage of the area where the nmRSEI correlated positively with temperature was 26.04%, mostly located in CLCA, the desertified grassland near the river network, and in the vicinity of Tengger Nuoer Lake. The results of the correlation analysis of the nmRSEI and precipitation and significance test showed that the percentage of area exhibiting a negative correlation between the nmRSEI and precipitation was 58.63%, mainly located north of the GLCA and CLCA. However, the percentage of area exhibiting a positive correlation between the nmRSEI and precipitation was 41.37%, mostly located in the CLCA and in the central part of the desertified steppe. The proportion of negative correlations between temperature and nmRSEI was higher than the proportion of positive correlations between precipitation and nmRSEI, indicating that the ecological quality of the study area was greatly affected by temperature. In addition, areas with a negative correlation with temperature were mainly distributed in the GLCA and BLCA, which indicates that the desertified steppe ecosystem is more sensitive to temperature responses.

Specifically, temperature promotes cultivated-land ecosystems. This is because the hydrological conditions of cultivated lands are significantly affected by human factors. When water supply is sufficient for vegetation growth, an increase in temperature accelerates photosynthesis and promotes vegetation growth. Temperature is negatively correlated with bare land and grassland, mainly because the region is dominated by desert grasslands. An increase in temperature aggravates the transpiration of vegetation leaves and leads to insufficient water acquisition, which affects vegetation growth. Precipitation has a positive effect on cultivated land and some areas of grassland in the study area because it can effectively replenish surface water, alleviate the degree of surface desiccation, and replenish the water needed for vegetation growth; however, it is stronger in the short term in areas with high desertification and low vegetation coverage. Soil erosion caused by precipitation negatively impacts ecological quality.

4.5.3. Driving effect of human factors on ecological indicators

Population density, sheep density, large livestock density (cattle, horses, donkeys, mules, and camels), and herbivorous livestock density information for Damao Banner from 1986 to 2018 were obtained from the statistical yearbook. The average value of nmRSEI, the average value of nmRSEI in the CLCA, and the average value of nmRSEI in the entire study area were analysed using Pearson correlation (Table 8). The results showed that, compared with other human factors, population density had a higher correlation with the average value of nmRSEI in the CLCA and the average value of nmRSEI in the entire study area. However, Pearson's correlation between these two factors failed to pass the significance test. Other factors with weak correlations did not pass the significance test. The results of the human factor analysis showed that the ecological quality of the Aibugai River Basin was affected by the population density to a certain extent, but the effect was limited. Although other human factors would disturb the ecological quality, none played a critical role. It must be noted that the above correlation analysis was performed between human factors and the average value of the nmRSEI, and errors caused by an uneven range of human activities

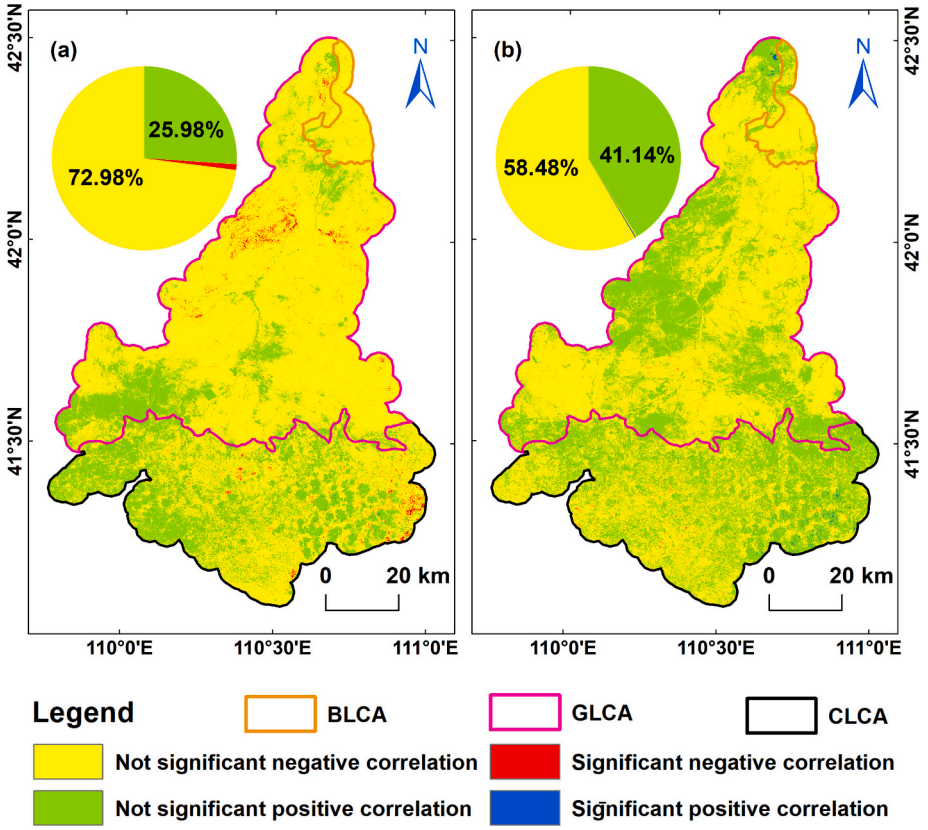

Fig. 12. Correlations of the new modified remote sensing ecological index (nmRSEI) with (a) temperature and (b) precipitation.

Table 8
Correlation analysis of humanistic factors and average new modified remote sensing ecological index (nmRSEI).

Humanistic factors	Avg. nmRSEI BLCA		Avg. nmRSEI GLCA		Avg. nmRSEI CLCA		Avg. nmRSEI	
	r	*P*	*r*	*P*	*r*	*P*	*r*	*P*
Population density (people/km^2)	0.058	0.883	−0.278	0.468	−0.471	0.201	−0.394	0.293
Sheep density (pcs/ km^2)	0.218	0.572	0.095	0.807	−0.173	0.656	−0.021	0.957
Large livestock density (pcs/km^2)	−0.067	0.865	0.055	0.888	0.319	0.403	0.187	0.631
Herbivorous livestock density (pcs/km^2)	0.236	0.541	0.117	0.764	−0.142	0.716	0.007	0.985

Note: *r* represents correlation coefficient; *P* represents significance; * indicates significant correlation at $P < 0.05$ level. Abbreviations: BLCA, bare land concentration area; GLCA, grassland concentration area; CLCA, cultivated land concentration area.

cannot be ruled out.

5. Discussion

5.1. Comparative analysis of RSEI and nmRSEI

(1) Data regarding CLCD data were introduced to verify the difference in the model's performance.

Considering that ecological quality is closely related to land cover type (Chen et al., 2022; Du et al., 2023), the performance differences between models can be indirectly verified by comparing the proportions of each ecological grade between the RSEI and nmRSEI under different land cover (Zheng et al., 2022). The land cover data selected in this study were obtained from the 30 m-year dataset publicly released by Yang Jie of Wuhan University and others (Yang and Huang, 2021). Owing to the lack of data from 1986 to 1989 in this dataset, we selected nine scenes of land-cover data from 1990 to 2022, corresponding to the time series of this research. In this dataset, the land use/land cover types included farmland, grassland, bare land, and impervious surfaces. Theoretically, when there is more vegetation, the ecological quality results assessed using the RSEI or nmRSEI will be better, and vice versa

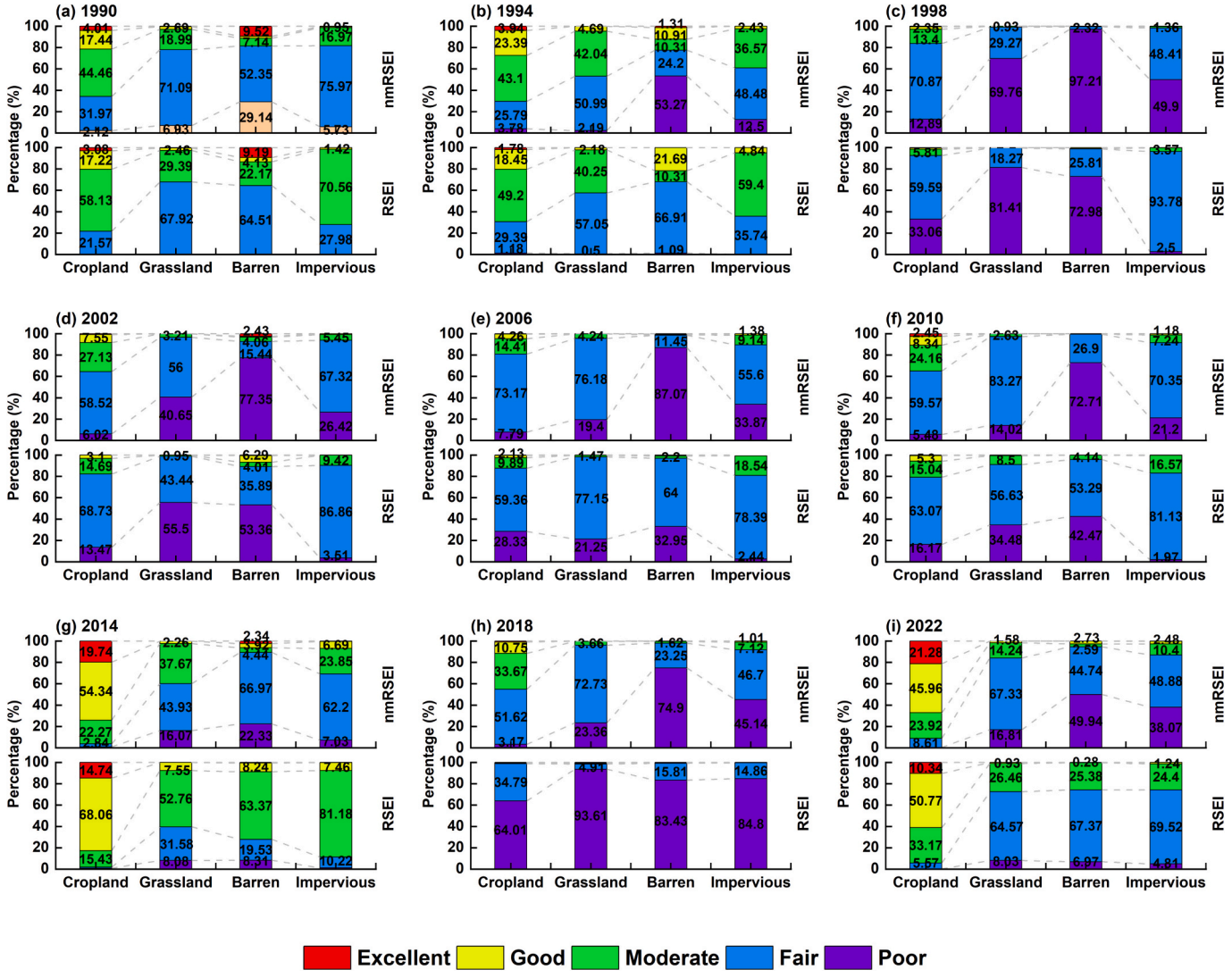

Fig. 13. Proportions of each ecological grade of remote sensing ecological index (RSEI) and new modified remote sensing ecological index (nmRSEI) of different land covers.

(Zheng et al., 2022). The proportions of each ecological grade for the different land cover types are shown in Fig. 13.

For different land cover types, the RSEI ecological grades shown as farmland and impervious surfaces are mainly 'fair' and 'moderate', and grassland and bare land are mostly 'poor' and 'fair'. The ecological grades of the nmRSEI shown as farmland are mainly 'fair' and 'moderate'; grassland and impervious surfaces are mostly 'Poor' and 'Fair'; bare land is mainly 'poor'. It can be seen that in farmland and grassland with higher vegetation coverage, the ecological grades of RSEI and nmRSEI are roughly similar. On bare land and impervious surfaces with low vegetation coverage, the nmRSEI can better reflect realistic ecological conditions. The RSEI was overestimated compared to the nmRSEI. This result is consistent with those of previous studies (Wang et al., 2023; Zheng et al., 2022).

(2) Data regarding NPP were introduced to verify differences in the model's performance.

The NPP of vegetation represents the dry matter mass obtained by green plants during photosynthesis and is a key parameter of the terrestrial ecosystem and surface carbon cycle (Zeng et al., 2023). As an important indicator of ecosystem functions and processes, NPP is highly sensitive to regional environmental changes and can be used as a basis for measuring regional ecological quality. Therefore, the performance difference between the RSEI and nmRSEI can be verified by comparing the intrinsic relationship between the two models and NPP. The trends in the timing averages of nmRSEI, RSEI, and NPP are shown in Fig. 14.

As MODerate-resolution Imaging Spectroradiometer NPP data were not available before 2000, a linear regression of the mean values of nmRSEI, RSEI, and NPP from 2002 to 2022 is presented in Fig. 14. The fitting results showed that all three types of data exhibited fluctuating upward trends within the time series. The fluctuation trends in mean NPP were consistent with those in both ecological indices, except in 2002 and 2022, when the fluctuation trend was opposite to those in the nmRSEI and RSEI.

The spatial distributions of RSEI from 1986 to 2022 and NPP from 2002 to 2022 in the study area are shown in Fig. A1 and Fig. A2, respectively. As shown in Fig. A1 and Fig. 7, the results of the ecological quality analysis using RSEI and nmRSEI differed greatly in BLCA and CLCA. However, the spatial heterogeneity of the RSEI and nmRSEI cannot be directly quantified using the spatial distribution of the NPP because of the different dimensions of the NPP and the two ecological indices. Therefore, in this study, NPP data were correlated with RSEI and nmRSEI, and the results are shown in Table 9.

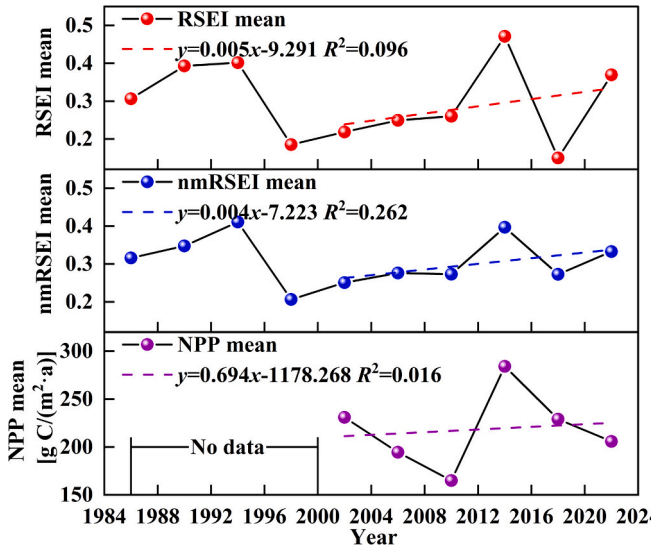

Fig. 14. Trends in the mean values of remote sensing ecological index (RSEI), new modified RSEI (nmRSEI), and net primary productivity (NPP).

As shown in Table 9, in the BLCA, the correlation coefficient between NPP and nmRSEI was greater than that between NPP and RSEI for all years except 2006 and 2022. In GLCA, the correlation coefficient between NPP and nmRSEI was greater than that between NPP and RSEI. In the CLCA, the correlation coefficient between NPP and nmRSEI was greater than that between NPP and RSEI for all years except 2014 and 2022. Based on the above results, it can be concluded that nmRSEI performs better than RSEI in the ecological assessment of arid and semi-arid areas.

5.2. Scientific and practical significance of nmRSEI

For conducting studies on ecological quality in arid and semi-arid areas, the selection of the greenness index for RSEIs was mainly concentrated on NDVI (Jiang et al., 2019; Qin et al., 2024; Wang et al., 2021b). It is undeniable that NDVI has the widest applicability among vegetation indices; however, the main problem with the use of NDVI is that in areas with low vegetation coverage, the soil background interferes with the extraction of the vegetation index and affects the accuracy of the index extraction (Huang et al., 2021). To overcome the above problems and accurately evaluate regional ecological quality, a few researchers have introduced SAVI in arid and semi-arid areas (Fan et al., 2023; Luo et al., 2023). This idea has a certain reference value, but the existing problem is that the soil adjustment coefficient L must be artificially determined in the SAVI, which determines the accuracy of the results of the SAVI-based analysis (Rhyma et al., 2020). Therefore, in this study, MSAVI was used instead of NDVI to construct the nmRSEI to avoid the need to determine the soil-regulated coefficient *L* when using SAVI. To test the rationality of using MSAVI instead of SAVI, Eq. (4) was used to calculate the S/N ratios of the two indices, and the results are shown in Fig. 15.

As shown in Fig. 15a–c, the S/N ratios of different land cover types were as follows: S/N_MSAVI bare land>S/N_SAVI bare land, S/N_MSAVI grassland>S/N_SAVI grassland, and S/N_MSAVI cultivated land>S/N_SAVI cultivated land. This indicates that MSAVI can relatively more effectively weaken the impact of the soil background on the greenness index extraction than SAVI. As shown in Fig. 15d, during the study period, the trend of the S/N ratios was as follows: S/N_MSAVI>S/N_SAVI. This further demonstrates that MSAVI can extract the greenness index of the study area relatively more accurately than SAVI.

In addition, the RSEI-based model does not consider the problem of soil salinisation in arid and semi-arid areas. This problem severely restricts the development of the regional ecological environment and economy (Cao et al., 2016; Zhang et al., 2019). Based on the actual situation, this study introduced the ratio SI-T (Allbed et al., 2014; Wang et al., 2019), which is adapted to evaluate the soil salt content in low vegetation coverage areas to reflect the degree of soil salinisation; thus, nmRSEI can more accurately reflect the ecological quality of the study area. This study also found that buildings and artificial surfaces only account for approximately 1.35% of the study area. It is unreasonable to use the original dryness index construction method to give 1/2 weight to the IBI. Therefore, IBI in the original dryness index was abandoned, and only SI was retained to characterise surface dryness.

In general, nmRSEI solves the applicability problem of RSEI in arid and semi-arid areas, enriches the remote sensing ecological index system, provides new ideas for ecological quality evaluation in arid and semi-arid areas, can provide ecological protection for arid and semi-arid areas and theoretical support for the realisation of the United Nations 2030 Sustainable Development Goals.

5.3. Comparison of nmRSEI and other comprehensive evaluation indices

Compared with existing ecological quality evaluation models for arid areas, this study has the following advantages. Yao et al. (2022)

Table 9
Correlation analysis between net primary productivity (NPP) and remote sensing ecological index (RSEI) and new modified RSEI (nmRSEI).

	BLCA		GLCA		CLCA	
Year	Correlation between NPP and nmRSEI	Correlation between NPP and RSEI	Correlation between NPP and nmRSEI	Correlation between NPP and RSEI	Correlation between NPP and nmRSEI	Correlation between NPP and RSEI
2002	0.915**	0.914**	0.906**	0.899**	0.906**	0.897**
2006	0.952**	0.962**	0.937**	0.912**	0.910**	0.890**
2010	0.983**	0.977**	0.955**	0.853**	0.926**	0.920**
2014	0.945**	0.911**	0.958**	0.952**	0.953**	0.962**
2018	0.972**	0.907**	0.956**	0.891**	0.933**	0.776**
2022	0.978**	0.980**	0.935**	0.930**	0.930**	0.947**

Note: ** indicates significant correlation at 0.001 level. Abbreviations: BLCA, bare land concentration area; GLCA, grassland concentration area; CLCA, cultivated land concentration area.

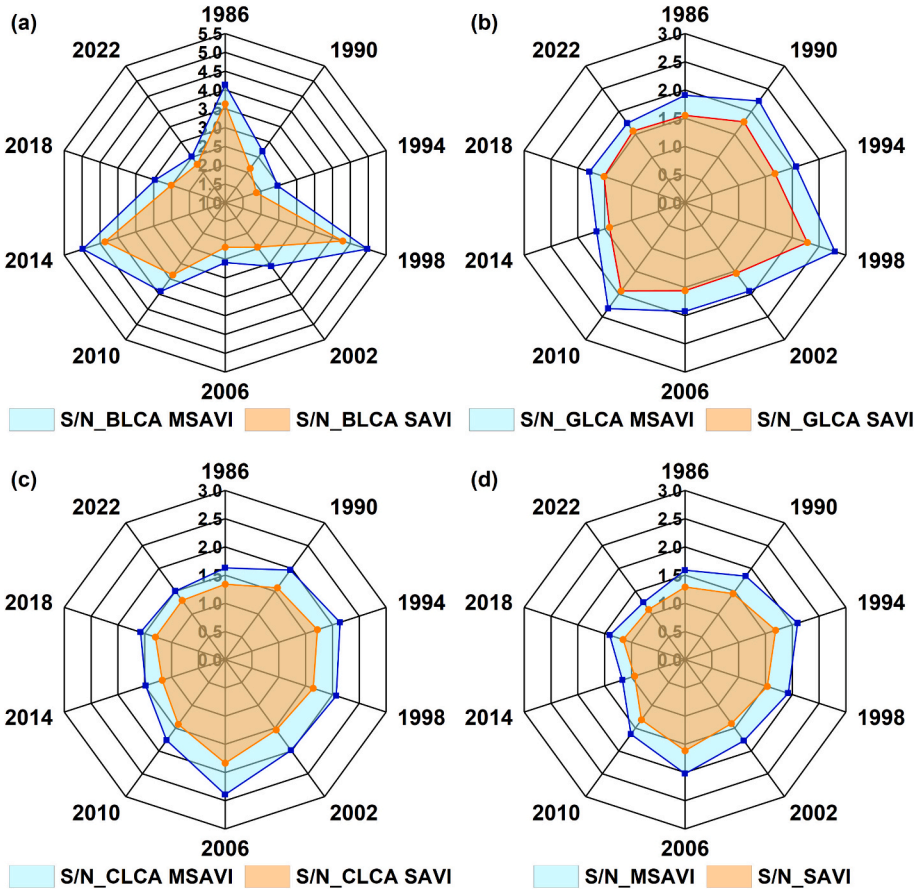

Fig. 15. Ratios of vegetation signal to soil noise calculated using SAVI and MSAVI in different years for different land cover areas. (a)–(c) Ratios of vegetation signal to soil noise calculated using SAVI and MSAVI in the BLCA, GLCA, and CLCA regions, respectively. (d) Ratios of vegetation signal to the soil noise of the whole study area. Abbreviations: SAVI, soil-adjusted vegetation index; MSAVI, modified soil-adjusted vegetation index; BLCA, bare land concentration area; GLCA, grassland concentration area; CLCA, cultivated land concentration area.

constructed an improved RSEI that couples greenness, humidity, heat, dryness, and salinity and enables the dynamic monitoring of ecological quality in the Hotan Oasis. Compared with our proposed nmRSEI, which introduces a dryness index consisting only of the construction index IBI, this dryness index inevitably leads to distortions in the extraction of the degree of surface drying in non-artificial surface areas. Combined with the results of the analysis presented in Section 4.1.1, it can be concluded that the extraction of the surface dryness index must consider the actual situation in the study area.

Zhao et al. (2023) constructed an MRSEI that, in contrast to the original RSEI, utilised the ratio of total regional precipitation to total potential evapotranspiration to represent humidity, used air temperature data to characterise surface temperature, and introduced a soil erosion indicator. Compared with our proposed nmRSEI, this index has a certain reference value, as it considers the erosive effects of precipitation and runoff on the soil; however, the use of air temperature to characterise the surface temperature leads to an underestimation of the results obtained compared to the actual situation (Li et al., 2023). Duo et al. (2023) proposed the MRSEI, which consists of the NDVI, WET, LST, NDBSI, and the DI. The DI introduced by the model was obtained from the Albedo-NDVI feature space, which can accurately extract information on soil desertification in arid areas and has a certain reference value. However, compared with the nmRSEI proposed in this study, this model also does not take into account the fact that the soil background in desertified areas will have an impact on NDVI extraction.

Qin et al. (2024) considered this issue when evaluating the ecological

quality of the middle reaches of the Yellow River, which utilised the kNDVI to replace the NDVI in the RSEI to improve the noise immunity of the greenness indicator. However, the S/N ratios of NDVI and kNDVI were not quantitatively compared in this study; therefore, the applicability of kNDVI in the ecological study of arid areas needs to be studied in depth.

Some researchers have constructed an improved vegetation health index (VHI) (Zheng et al., 2022), which is composed of a vegetation condition index (VCI) and a temperature condition index (TCI) and can be used to monitor the drought stress caused by vegetation. Compared to the nmRSEI proposed in this study, this index has the advantage of considering the physical characteristics of organisms and climatic conditions. However, it can only be used to evaluate the drought status of a region and cannot reflect the overall ecological quality of the region.

5.4. External factors affecting ecological quality

(1) Reliability assessment of the meteorological data.

When collecting meteorological data for this study, we prioritised meteorological station data; however, the fewer and sparsely distributed meteorological stations near the study area could not meet the interpolation requirements. Meteorological station data are insufficient for exploring the drivers of meteorological factors affecting ecological quality at the pixel-by-pixel level. The distribution of meteorological stations in the study area is shown in Fig. 1d. Therefore, in this study, we considered the use of meteorological data products to address the above issues, and ERA-5 data and China 1 km resolution meteorological data have attracted our attention. To check the reliability of both datasets, the data measured at the Mandula and Damao Banner meteorological stations near the study area were selected to evaluate the ERA5 and China 1 km resolution meteorological data. First, annual precipitation and average annual temperature from 1986 to 2018 (2022 meteorological data points were incomplete) were obtained for both meteorological stations. Subsequently, based on the latitudes and longitudes of the two meteorological stations, the annual precipitation and annual mean temperature values corresponding to the 1 km resolution meteorological data of ERA-5 and China 1 km resolution meteorological data from 1986 to 2018 were extracted, respectively. Scatterplot analysis of the meteorological station data with the two meteorological data products was performed separately, and the results are shown in Fig. 16.

As shown in Fig. 16a and c, the ERA5 precipitation data had a linear relationship with the meteorological station precipitation data and were significantly correlated ($P < 0.05$). However, the 1 km resolution precipitation data had a poor linear relationship and low correlation ($P > 0.05$) with the meteorological station precipitation data, while its RMSE was larger than that of the ERA5 precipitation data. As can be seen from Fig. 16b and Fig. 16d, both the ERA5 temperature data and the 1 km resolution temperature data have a good linear relationship with the meteorological station temperature data; the correlation and significance between the ERA5 temperature data and the meteorological station temperature data is high, and the RMSE is low. From the results of the above comparative analysis, it can be seen that the ERA5 meteorological data are more reliable than the China 1 km resolution meteorological data.

(2) Impact of meteorological factors on ecological quality.

From the spatial distribution of the nmRSEI, we can see that as latitude increases, the ecological quality gradually deteriorates. This is because the upper reaches of the southern Aibugai River are close to the 400 mm equal precipitation line, and the northern downstream area is close to the 200 mm equal precipitation line. Effective precipitation in the upper reaches alleviates surface drought conditions to a certain extent. In addition, the ecological quality of the study area significantly deteriorated between 1986 and 2002. In 1998, ecological quality was the worst. This is because rural construction in Damao Banner experienced rapid development from 1979 to 2002. The state of the human-land system has undergone significant changes. The implementation of a series of ecological management projects, such as the Returning Farmland to Forest and Grassland Project in 2002, Beijing-Tianjin Sandstorm Source Project, and Comprehensive Grazing Ban, has significantly improved the ecological quality of the study area (Li et al., 2020; Li et al., 2021).

While exploring the impact of external factors on ecological quality, we found that temperature was negatively correlated with nmRSEI each year, whereas precipitation was positively correlated. However, when exploring the spatial differences in the impacts of temperature and precipitation on the ecological quality of the study area at the pixel-by-pixel level, we found that temperature has a certain promoting effect on areas where cultivated land is concentrated. This is because soil moisture conditions in cultivated land are affected by both precipitation and artificial irrigation. When there is sufficient moisture, the temperature promotes photosynthesis of vegetation (Mao et al., 2012), which results in significantly better growth than in desert grassland areas. In addition, although precipitation can effectively alleviate the degree of surface desiccation in arid and semi-arid areas, it should be noted that short-term heavy precipitation may lead to the occurrence of secondary disasters such as water and soil erosion (Wang et al., 2022c), thereby negatively affecting ecological quality.

5.5. Limitations and prospects

In this study, a series of explorations based on the RSEI were performed, and an improved remote sensing ecological index, nmRSEI, was constructed, which solved the applicability problem of RSEI for ecological quality evaluation in arid and semi-arid areas, further enriching the remote sensing ecological indices for arid and semi-arid areas and providing new ideas for regional ecological quality evaluation. However, there remains scope for improvement and directions for further research.

(1) Owing to the large span of the study, limited by the impact of cloud coverage and the satellite revisit period, although the selected data are from a period of vigorous vegetation growth, the influence of time differences cannot be avoided. Subsequently, the synthesis of the mean values of each indicator component during the vigorous growth period was used to construct the nmRSEI. We used the average ecological quality of the entire vigorous growth period to overcome the influence of time differences on the experimental results.
(2) Remote sensing data must be selected to ensure low cloud cover and good data quality. The clouds can lead to blurring and missing surface observations, affecting the real surface reflectivity information of ground objects, which will lead to a lower inversion accuracy of the index component used to construct the nmRSEI and affect the accuracy of the nmRSEI results. In future research, we will attempt to introduce synthetic aperture radar data to build an ecological quality evaluation model based on the collaborative processing of active and passive remotely sensed data to overcome the problem of cloud cover.
(3) The IBI in the original dryness index was abandoned, and only SI was selected to characterise the surface drying situation. This method can be applied to 98.65% of the study area, except the artificial surface, but there is a certain distortion in the 1.35% area of the artificial surface coverage. This is a limitation of the present study. In subsequent research, the calculation of the IBI was divided into three steps. First, the artificial surface and building area were extracted, the IBI was calculated for these areas, the SI for the other areas was calculated, and the two indices (IBI and SI) were combined to achieve a relatively more accurate characterisation of surface drying.

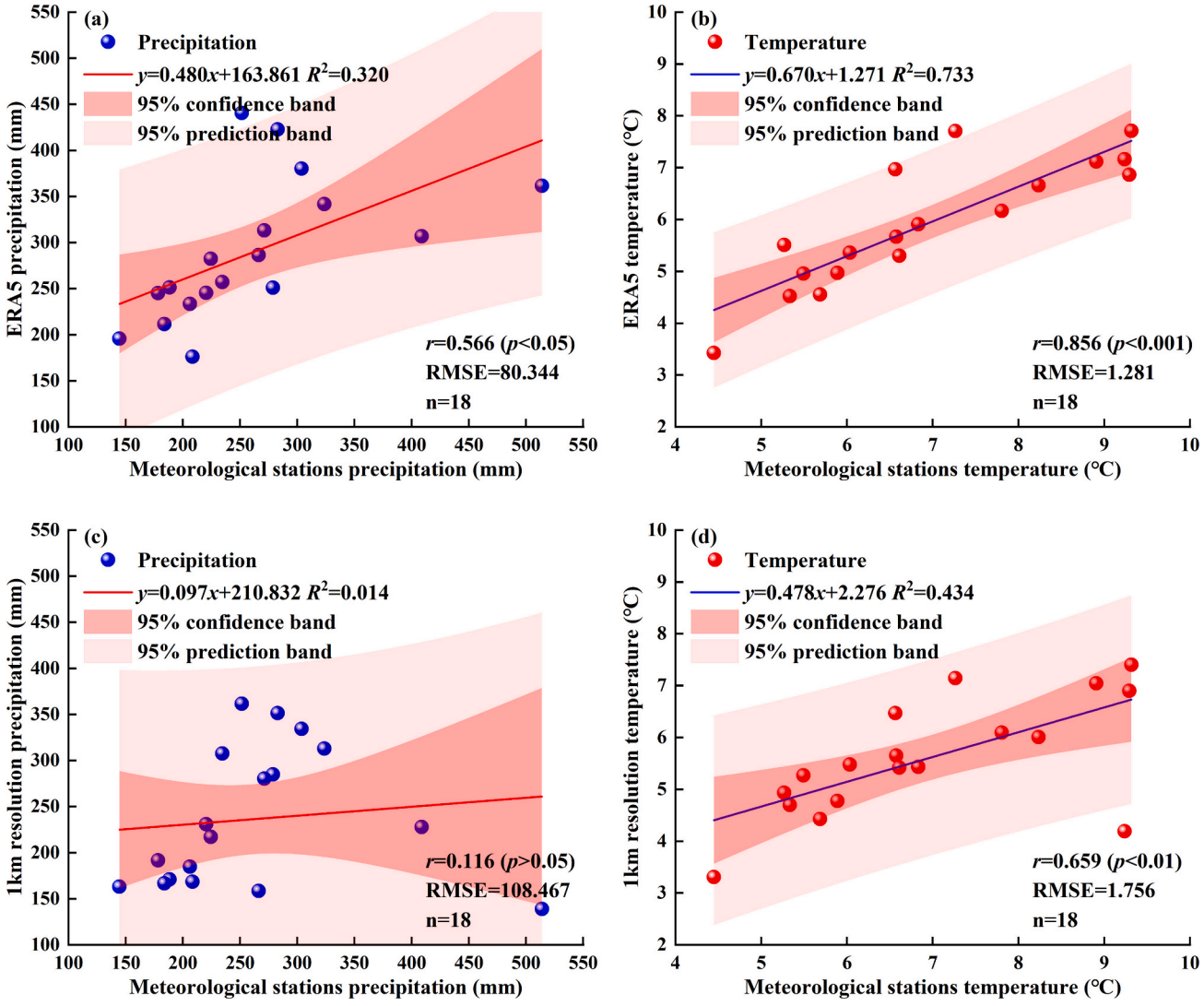

Fig. 16. Reliability assessment of meteorological data. Notes: r represents correlation; p represents significance; RMSE represents root mean square error; n represents the number of scatters; R^2 represents the goodness of fit.

6. Conclusions

In this study, long-term remotely sensed data and RSEI were used, and nmRSEI was proposed and tested in the Aibugai River Basin, which solves the problem of the non-applicability of the existing RSEIs to arid and semi-arid areas. The main conclusions of this study are as follows:

(1) The S/N ratios calculated using MSAVI were higher than those calculated using NDVI for all analysed years, indicating that using MSAVI to replace NDVI can effectively weaken the interference of the soil background in the extraction of greenness indicators. As the percentage of buildings and human-made surfaces in the study area is only approximately 1.35%, the initial dryness index will lead to an underestimation of the desiccation degree, and the new dryness index constructed only with SI can satisfy 98.65% of the area except buildings and artificial surfaces. The introduced salinity index was highly negatively correlated with the nmRSEI, and the introduction of this index into the model could more accurately evaluate the ecological quality of the ASR.
(2) A comparative analysis of the EVs, contribution rates, and scatter plots of the RSEI- and nmRSEI-based models showed that the nmRSEI-based model can better integrate the information contained in each ecological component and is more stable and reliable. In addition, the results of the ecological quality evaluation of the two models were compared with third-party data (CLCD, NPP and EI), which verified the credibility of nmRSEI for ecological quality evaluation.
(3) From 1986 to 2022, the ecological quality showed a periodic change; that is, from 1986 to 1998, the ecological quality showed a decreasing trend; from 1998 to 2014, the ecological quality showed an improvement trend; and from 2014 to 2022, the ecological quality showed a declining trend again. The T–S trend analysis combined with the M–K method showed that the dominant ecological quality from 1986 to 2022 belonged to the 'no change' category, but the overall trend revealed the dominance of the 'steady and degraded' category.
(4) The year-by-year correlation analysis showed that the nmRSEI was positively correlated with precipitation and negatively correlated with temperature. The results of the time-series correlation analysis showed that temperature was the main factor controlling the ecological quality in the study area. Although human factors can disturb the ecological quality, they do not play a decisive role.

The proposed nmRSEI can more scientifically monitor the dynamic changes in ecological quality in arid/semiarid areas, accurately reveal the changing trends of ecological quality, and further enrich remote sensing ecological indices, which can provide theoretical support for precise regional ecological governance and regional sustainable development.

Funding

This work was funded by National Natural Science Foundation of China (U21A20108), Open Project Program of Yazhou Bay Innovation Institute of Hainan Tropical Ocean University (2022CXYKFKT03), Hainan Provincial Natural Science Foundation of China (423MS120), funding of Hainan Academy of Ocean and Fisheries Sciences (KYL-2023-01) and Provincial-level project of Hainan Province, Hainan Academy of Marine and Fishery Sciences (KYL-2023-01).

Author contributions

All authors contributed to the study conception and design. Conceptualization: Chao Ma; Data curation: Haobin Zhang; Formal analysis: Haobin Zhang, Chao Ma; Funding acquisition: Chao Ma; Investigation: Haobin Zhang; Methodology: Chao Ma, Haobin Zhang; Project Administration: Chao Ma; Software: Haobin Zhang; Supervision: Chao Ma, Pei Liu; Validation: Haobin Zhang, Pei Liu; Visualization: Haobin Zhang; Writing–original draft: Chao Ma & Haobin Zhang; Writing–review & editing: Pei Liu. All authors read and approved the final manuscript.

Declaration of competing interest

The authors declare that they have no known competing financial interests or personal relationships that could have appeared to influence the work reported in this paper.

Data availability

Landsat data used in this study is available from the USGS website (https://earthexplorer.usgs.gov/) and Geospatial Data Cloud (https://www.gscloud.cn/). DEM data provided by CGIAR-CSI were selected (https://cgiarcsi.community/). Meteorological data from the ERA5 reanalysis dataset (https://cds.climate.copernicus.eu/). Land cover data comes from the global land cover data provided by GlobeLand30 (http://www.globallandcover.com/), with a spatial resolution of 30 m × 30 m. The humanistic data comes from the Damao Banner Statistical Yearbook (https://data.cnki.net/) and Statistical Bulletin (http://www.dmlhq.gov.cn/) of Baotou City, Inner Mongolia.

Appendix A

Spatial distribution of RSEI from 1986 to 2022 (Fig. A1) and spatial distribution of NPP from 2002 to 2022 (Fig. A2) in the study area.

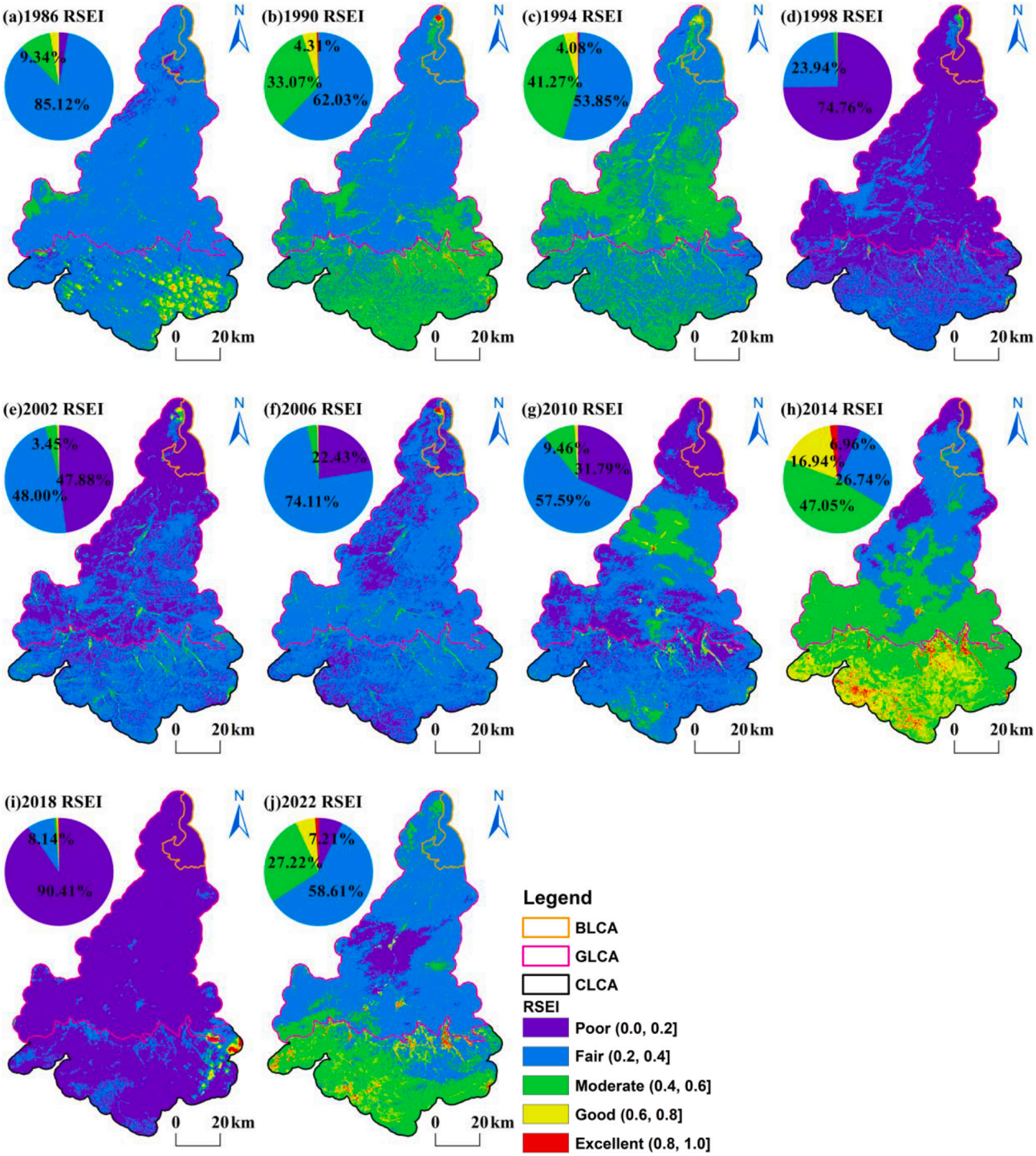

Fig. A1. The RSEI level distribution maps of AiBuGai River Basin from 1986 to 2022.

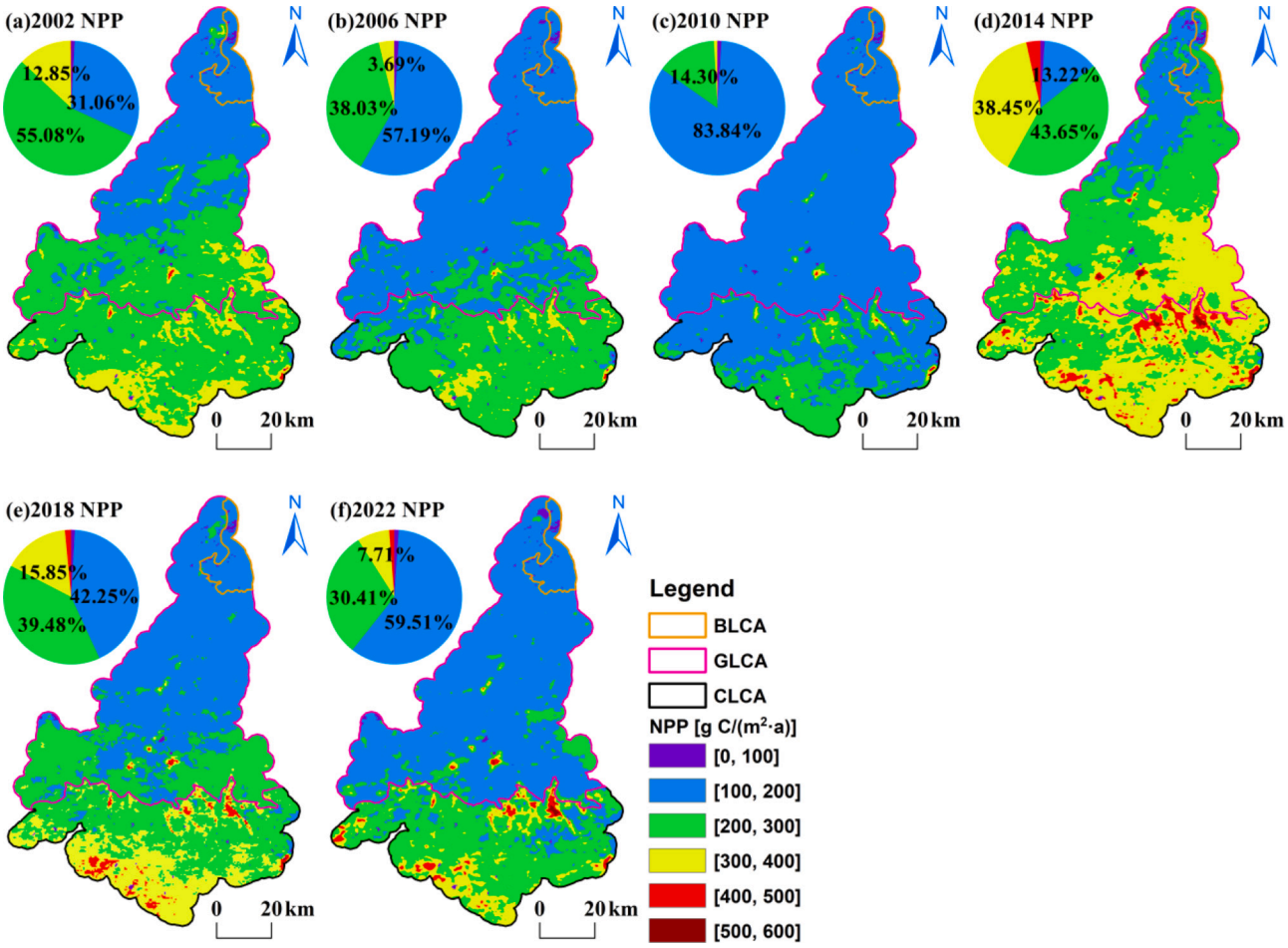

Fig. A2. Spatial distribution of NPP in the study area from 2002 to 2022.

References

Allbed, A., Kumar, L., Aldakheel, Y.Y., 2014. Assessing soil salinity using soil salinity and vegetation indices derived from IKONOS high-spatial resolution imageries: applications in a date palm dominated region. Geoderma 230–231, 1–8. https://doi.org/10.1016/j.geoderma.2014.03.025.

Cai, Z., Zhang, Z., Zhao, F., Guo, X., Zhao, J., Xu, Y., Liu, X., 2023. Assessment of eco-environmental quality changes and spatial heterogeneity in the Yellow River Delta based on the remote sensing ecological index and geo-detector model. Ecol. Inform. 77, 102203 https://doi.org/10.1016/j.ecoinf.2023.102203.

Cao, L., Ding, J., Zeti, H., Su, W., Ning, J., Miao, C., Li, H., 2016. Extraction and modeling of regional soil salinization based on data from GF-1 satellite. Acta Pedol. Sin. 53, 1399–1409. https://doi.org/10.11766/trxb201601270650.

Cao, Z., Zhu, T., Cai, X., 2023. Hydro-agro-economic optimization for irrigated farming in an arid region: the Hetao Irrigation District, Inner Mongolia. Agric. Water Manag. 277, 108095 https://doi.org/10.1016/j.agwat.2022.108095.

Chander, G., Markham, B.L., Helder, D.L., 2009. Summary of current radiometric calibration coefficients for Landsat MSS, TM, ETM+, and EO-1 ALI sensors. Remote Sens. Environ. 113, 893–903. https://doi.org/10.1016/j.rse.2009.01.007.

Chen, J., John, R., Sun, G., Fan, P., Henebry, G.M., Fernández-Giménez, M.E., Zhang, Y., Park, H., Tian, L., Groisman, P., Ouyang, Z., Allington, G., Wu, J., Shao, C., Amarjargal, A., Dong, G., Gutman, G., Huettmann, F., Lafortezza, R., Crank, C., Qi, J., 2018. Prospects for the sustainability of social-ecological systems (SES) on the Mongolian plateau: five critical issues. Environ. Res. Lett. 13 https://doi.org/10.1088/1748-9326/aaf27b.

Chen, C., He, X., Fu, J., Chu, Y., 2019. A method of flood submerging area extraction for farmland based on tasseled cap transformation from remote sensing images. Geomatics Inf. Sci. Wuhan Univ. 44, 1560–1566. https://doi.org/10.13203/j.whugis20180067.

Chen, Z., Chen, J., Zhou, C., Li, Y., 2022. An ecological assessment process based on integrated remote sensing model: a case from Kaikukang-Walagan District, greater Khingan range, China. Ecol. Inform. 70, 101699 https://doi.org/10.1016/j.ecoinf.2022.101699.

Crist, E.P., 1985. A TM tasseled cap equivalent transformation for reflectance factor data. Remote Sens. Environ. 17, 301–306. https://doi.org/10.1016/0034-4257(85)90102-6.

Dai, Y., Guan, Y., Liu, M., Zhang, Q., He, X., 2022. Dynamic monitoring and evaluation of ecological environment quality in alar reclamation area from 1990 to 2020. Bull. Soil Water Conserv. 42, 122–128. https://doi.org/10.13961/j.cnki.stbctb.2022.02.017.

Du, L., Dong, C., Kang, X., Qian, X., Gu, L., 2023. Spatiotemporal evolution of land cover changes and landscape ecological risk assessment in the Yellow River Basin, 2015–2020. J. Environ. Manag. 332, 117149 https://doi.org/10.1016/j.jenvman.2022.117149.

Duo, L., Wang, J., Zhang, F., Xia, Y., Xiao, S., He, B.J., 2023. Assessing the spatiotemporal evolution and drivers of ecological environment quality using an enhanced remote sensing ecological index in Lanzhou City, China. Remote Sens. 15 https://doi.org/10.3390/rs15194704.

Fan, X., Yu, H., Tiando, D.S., Rong, Y., Luo, W., Eme, C., Ou, S., Li, J., Liang, Z., 2021. Impacts of human activities on ecosystem service value in arid and semi-arid ecological regions of China. Int. J. Environ. Res. Public Health 18. https://doi.org/10.3390/ijerph182111121.

Fan, Q., Shi, Y., Song, X., Cong, N., 2023. Study on factors affecting remote sensing ecological quality combined with Sentinel-2. Remote Sens. 15 https://doi.org/10.3390/rs15082156.

Geng, J., Yu, K., Xie, Z., Zhao, G., Ai, J., Yang, L., Yang, H., Liu, J., 2022. Analysis of spatiotemporal variation and drivers of ecological quality in Fuzhou based on RSEI. Remote Sens. 14 https://doi.org/10.3390/rs14194900.

Goward, S.N., Xue, Y., Czajkowski, K.P., 2002. Evaluating land surface moisture conditions from the remotely sensed temperature/vegetation index measurements: an exploration with the simplified simple biosphere model. Remote Sens. Environ. 79, 225–242. https://doi.org/10.1016/S0034-4257(01)00275-9.

Guo, B., Zhang, J., Xu, T., Song, Y., Liu, M., Dai, Z., 2022. Assessment of multiple precipitation interpolation methods and uncertainty analysis of hydrological models in Chaohe River basin, China. Water SA 48, 324–334. https://doi.org/10.17159/wsa/2022.v48.i3.3884.

Han, Z., Zhang, Y., Wang, H., Ji, G., Liang, W., Jiao, R., 2020. Temporal and spatial distribution characteristics of isotope content in surface water-soil water-ground

water of Dalhan Maomingan joint banner. Water Sav. Irrig. 74–80 doi:1007–4929 (2020) 07–0074-07.
Hersbach, H., Bell, B., Berrisford, P., Hirahara, S., Horányi, A., Muñoz-Sabater, J., Nicolas, J., Peubey, C., Radu, R., Schepers, D., Simmons, A., Soci, C., Abdalla, S., Abellan, X., Balsamo, G., Bechtold, P., Biavati, G., Bidlot, J., Bonavita, M., De Chiara, G., Dahlgren, P., Dee, D., Diamantakis, M., Dragani, R., Flemming, J., Forbes, R., Fuentes, M., Geer, A., Haimberger, L., Healy, S., Hogan, R.J., Hólm, E., Janisková, M., Keeley, S., Laloyaux, P., Lopez, P., Lupu, C., Radnoti, G., de Rosnay, P., Rozum, I., Vamborg, F., Villaume, S., Thépaut, J.N., 2020. The ERA5 global reanalysis. Q. J. R. Meteorol. Soc. 146, 1999–2049. https://doi.org/10.1002/qj.3803.
Huang, J., Ma, J., Guan, X., Li, Y., He, Y., 2019. Progress1. Yin, Y.; Ma, D.; Wu, S. Enlargement of the semi-arid region in China from 1961 to 2010. Clim. Dyn. 2019, 52, 509–521, doi:10.1007/s00382-018-4139-x. In semi-arid climate change studies in China. Adv. Atmos. Sci. 36, 922–937. https://doi.org/10.1007/s00376-018-8200-9.
Huang, S., Tang, L., Hupy, J.P., Wang, Y., Shao, G., 2021. A commentary review on the use of normalized difference vegetation index (NDVI) in the era of popular remote sensing. J. For. Res. 32, 1–6. https://doi.org/10.1007/s11676-020-01155-1.
Jarvis, A., Guevara, E., Reuter, H.I., Nelson, A.D., 2008. Hole-filled SRTM for the globe: version 4: data grid.
Jia, H., Yan, C., Xing, X., 2021. Evaluation of eco-environmental quality in qaidam basin based on the ecological index (MRSEI) and GEE. Remote Sens. 13 https://doi.org/10.3390/rs13224543.
Jiang, C., Wu, L., Liu, D., Wang, S., 2019. Dynamic monitoring of eco-environmental quality in arid desert area by remote sensing: taking the Gurbantunggut Desert China as an example. Chin. J. Appl. Ecol. 30, 877–883. https://doi.org/10.13287/j.1001-9332.201903.008.
Jun, C., Ban, Y., Li, S., 2014. Open access to earth land-cover map. Nature 514, 434. https://doi.org/10.1038/514434c.
Kang, X., Cao, J., Chen, C., Yang, J., Wang, J., 2020. Analysis of long-term vegetation change in Ningxia with different trend methods. Bull. Surv. Mapp. 23–27 https://doi.org/10.13474/j.cnki.11-2246.2020.0348.
Li, J., Cui, L., Yan, X., Yang, Z., Dong, J., Deng, X., 2019. Comparative analysis of long-term trends on fraction of vegetation coverage in grassland mining area. Bull. Surv. Mapp. 130–134. +157. 10.13474/j.cnki.11-2246.2019.0267.
Li, W., Lin, H., Kuang, W., 2020. Adaptability evolution mechanism of farmers and herdsmen of village in north agricultural-pastoral ecotone: take Damao banner in Inner Mongolia as an example. Econ. Geogr. 40, 150–163. https://doi.org/10.15957/j.cnki.jjdl.2020.01.017.
Li, W., Kuang, W., Lv, J., Zhao, Z., 2021. Adaptive evolution mechanism of rural human-land system in farming-and-pastoral areas of northern China. Acta Geograph. Sin. 76, 487–502. https://doi.org/10.11821/dlxb202102017.
Li, D., Duan, K., Shi, P., Li, S., Shang, Y., Zhang, Z., 2022. Vertical variation of precipitation in the central Qinling Mountains. Acta Geograph. Sin. 77, 1762–1774. https://doi.org/10.11821/dlxb202207013.
Li, Y., Li, Z.L., Wu, H., Zhou, C., Liu, X., Leng, P., Yang, P., Wu, W., Tang, R., Shang, G.F., Ma, L., 2023. Biophysical impacts of earth greening can substantially mitigate regional land surface temperature warming. Nat. Commun. 14, 1–12. https://doi.org/10.1038/s41467-023-35799-4.
Liu, C., Liu, J., Zhang, Q., Ci, H., Gu, X., Gulakhmadov, A., 2022a. Attribution of NDVI dynamics over the globe from 1982 to 2015. Remote Sens. 14, 1–17. https://doi.org/10.3390/rs14112706.
Liu, Y., Zhang, Q., Liu, J., Guan, H., Meng, F., 2022b. Temporal and spatial characteristics of fractional vegetation coverage and its response to climatic factors in southern Xinjiang in recent 20 years: A case of Taxkorgan Tajik Autonomous County. Arid L. Geogr. 45, 1481–1489. https://doi.org/10.12118/j.issn.1000-6060.2021.606.
Liu, L., Xie, Y., Zhu, B., Song, K., 2024. Rice leaf chlorophyll content estimation with different crop coverages based on Sentinel-2. Ecol. Inform. 81, 102622 https://doi.org/10.1016/j.ecoinf.2024.102622.
Lu, J., Zhang, X., Ye, P., Wu, H., Wang, Tao, 2020. Remote sensing monitoring of salinization in Hetao irrigation district based on SI-MSAVI feature space. Remote Sens. L. Resour. 32, 169–175. https://doi.org/10.6046/gtzyyg.2020.01.23.
Luo, R., Wang, H., Wang, C., 2023. Ecological quality evaluation of Gulang County in Gansu Province based on improved remote sensing ecological index. Arid L. Geogr. 46, 539–549. https://doi.org/10.12118/j.issn.1000–6060.2022.322.
Mao, D., Wang, Z., Luo, L., Yang, S., 2012. Correlation analysis between NDVI and climate in China based on AVHRR and GIMMS data sources. Remote Sens. Technol. Appl. 27, 77–85.
Ministry of Ecology and Environment of the People''s Republic of China, 2015. Technical Criterion for Ecosystem Status Evaluation: HJ 192–2015. Quality and Standards Publishing & Media Co, Ltd, Beijing.
Pan, X., 2020. Inversion and Spatiotemporal Evoluation of Soil Salinity in Coastal Plain. Hebei Agric. Univ.
Qi, J., Chehbouni, A., Huete, A.R., Kerr, Y.H., Sorooshian, S., 1994. A modified soil adjusted vegetation index. Remote Sens. Environ. 48, 119–126. https://doi.org/10.1016/0034-4257(94)90134-1.
Qin, G., Wang, N., Wu, Y., Zhang, Z., Meng, Z., Zhang, Y., 2024. Ecological informatics spatiotemporal variations in eco-environmental quality and responses to drought and human activities in the middle reaches of the Yellow River basin, China from 1990 to 2022. Ecol. Inform. 81, 102641 https://doi.org/10.1016/j.ecoinf.2024.102641.
Rhyma, P.P., Norizah, K., Hamdan, O., Faridah-Hanum, I., Zulfa, A.W., 2020. Integration of normalised different vegetation index and soil-adjusted vegetation index for mangrove vegetation delineation. Remote Sens. Appl. Soc. Environ. 17, 100280 https://doi.org/10.1016/j.rsase.2019.100280.
Running, S., Zhao, M., 2021. MODIS/Terra Net Primary Production Gap-Filled Yearly L4 Global 500m SIN Grid V061. distributed by NASA EOSDIS Land Processes Distributed Active Archive Center. https://doi.org/10.5067/MODIS/MOD17A3HGF.061. Accessed 2024-04-12.
Song, Y., Guo, Z., Lu, Y., Liao, Z., Xu, X., 2017. An ecological vulnerability evaluation method for arid pasturing areas based on the SWAT model: a case study in the Aibugai Basin. Acta Ecol. Sin. 37, 3805–3815. https://doi.org/10.5846/stxb201604190737.
Tang, H., Wang, X., Chen, F., Jiang, L., He, C., Long, A., 2022. Simulation of Manas River runoff based on ERA5-land dataset. Earth Sci. 29, 271–283. https://doi.org/10.13745/j.esf.sf.2022.1.50.
Wang, F., Yang, S., Yang, W., Yang, X., Jianli, D., 2019. Comparison of machine learning algorithms for soil salinity predictions in three dryland oases located in Xinjiang Uyghur autonomous region (XJUAR) of China. Eur. J. Remote Sens. 52, 256–276. https://doi.org/10.1080/22797254.2019.1596756.
Wang, D., Yang, C., Zheng, Y., Xiao, X., Zhao, L., Zhenghong, C., 2021a. Estimation of mitigation effect of sponge City reconstruction on heat island effect. Resour. Environ. Yangtze Basin 30, 968–975. https://doi.org/10.11870/cjlyzyyhj202104019.
Wang, J., Liu, D., Ma, J., Cheng, Y., Wang, L., 2021b. Development of a large-scale remote sensing ecological index in arid areas and its application in the Aral Sea basin. J. Arid. Land 13, 40–55. https://doi.org/10.1007/s40333-021-0052-y.
Wang, J., Ding, J., Zhang, Z., 2022a. Change of ecological environment in Turpan and Hami cities based on remote sensing ecology index. Arid L. Geogr. 45, 1591–1603. https://doi.org/10.12118/j.issn.1000-6060.2022.346.
Wang, X., Li, T., Ikhumhen, H.O., Sá, M.R., 2022b. Spatio-temporal variability and persistence of PM2.5 concentrations in China using trend analysis methods and Hurst exponent. Atmos. Pollut. Res. 13, 101274 https://doi.org/10.1016/j.apr.2021.101274.
Wang, F., Li, W., Lin, Y., Nan, X., Hu, Z., 2022c. Spatiotemporal pattern and driving forces analysis of ecological environmental quality in typical ecological areas of the Yellow River Basin from 1990 to 2020. Environ. Sci. 1–13 https://doi.org/10.13227/j.hjkx.202206029.
Wang, X., Zhang, S., Zhao, X., Shi, S., Xu, L., 2023. Exploring the relationship between the eco-environmental quality and urbanization by utilizing sentinel and Landsat data: a case study of the Yellow River Basin. Remote Sens. 15 https://doi.org/10.3390/rs15030743.
Wen, X., Chen, X., Xu, H., 2022. Ecological evaluation of cities in southern Beijing suburbs based on remote sensing ecological index: taking Zhuozhou City and Gu'an county as examples. J. Fuzhou Univ. Nat. Sci. Ed. 50, 286–292. https://doi.org/10.7631/issn.1000-2243.21021.
Xu, H., 2013. A remote sensing urban ecological index and its application. Acta Ecol. Sin. 33, 7853–7862. https://doi.org/10.5846/stxb201208301223.
Xu, N., 2021. Research of ERA5 Daily-Scale Precipitation Prediction Method Based on LSTM Algorithm. Nanjing Univ. Posts Telecommun. https://doi.org/10.27251/d.cnki.gnjdc.2021.000786.
Xu, H., Deng, W., 2022. Rationality analysis of MRSEI and its difference with RSEI. Remote Sens. Technol. Appl. 37, 1–7. https://doi.org/10.11873/j.issn.1004-0323.2022.1.0001.
Xu, T., Li, Y., Wang, S., Jiang, N., 2022. Improved tropospheric delay model for China using RBF neural network and meteorological data. Acta Geod. Cartogr. Sin. 51, 1690–1707. https://doi.org/10.11947/j.AGCS.2022.20210480.
Xu, H., Duan, W., Deng, W., Lin, M., 2022a. RSEI or MRSEI? Comment on Jia et al. Evaluation of eco-environmental quality in Qaidam Basin Based on the Ecological Index (MRSEI) and GEE. Remote Sens. 2021, 13, 4543. Remote Sens. 14 https://doi.org/10.3390/rs14215307.
Yang, J., Huang, X., 2021. The 30m annual land cover dataset and its dynamics in China from 1990 to 2019. Earth Syst. Sci. Data 13, 3907–3925. https://doi.org/10.5194/essd-13-3907-2021.
Yang, Y., Li, H., 2023. Spatiotemporal dynamic decoupling states of eco-environmental quality and land-use carbon emissions: a case study of Qingdao City, China. Ecol. Inform. 75, 101992 https://doi.org/10.1016/j.ecoinf.2023.101992.
Yang, H., Xu, W., Yu, J., Xie, X., Xie, Z., Lei, X., Wu, Z., Ding, Z., 2023. Exploring the impact of changing landscape patterns on ecological quality in different cities: a comparative study among three megacities in eastern and western China. Ecol. Inform. 77, 102255 https://doi.org/10.1016/j.ecoinf.2023.102255.
Yao, K., Halike, A., Chen, L., Wei, Q., 2022. Spatiotemporal changes of eco-environmental quality based on remote sensing-based ecological index in the Hotan Oasis, Xinjiang. J. Arid Land 14, 262–283. https://doi.org/10.1007/s40333-022-0011-2.
Yin, Y., Ma, D., Wu, S., 2019. Enlargement of the semi-arid region in China from 1961 to 2010. Clim. Dyn. 52, 509–521. https://doi.org/10.1007/s00382-018-4139-x.
Yu, Y., Song, F., Zhang, S., 2022a. Quantitative analysis of temporal and spatial changes of NDVI and its driving factors in Henan province from 2000 to 2020. Ecol. Environ. Sci. 31, 1939–1950. https://doi.org/10.16258/j.cnki.1674-5906.2022.10.002.
Yu, F., Zhu, S., Zhang, G., Zhu, J., Zhang, N., Yongming, X., 2022b. A downscaling method for land surface air temperature of ERA5 reanalysis dataset under complex terrain conditions in mountainous areas. J. Geogr. Sci. 24, 750–765. https://doi.org/10.12082/dqxxkx.2022.210386.
Zeng, J., Zhou, T., Wang, Q., Xu, Y., Lin, Q., Zhang, Y., Wu, X., Zhang, J., Liu, X., 2023. Spatial patterns of China's carbon sinks estimated from the fusion of remote sensing and field-observed net primary productivity and heterotrophic respiration. Ecol. Inform. 76, 102152 https://doi.org/10.1016/j.ecoinf.2023.102152.

Zhang, Z., Wei, G., Yao, Z., Tan, C., Wang, X., Han, J., 2019. Soil salt inversion model based on UAV multispectral remote sensing. Trans. Chinese Soc. Agric. Mach. 50, 151–160. https://doi.org/10.6041/j.issn.1000-1298.2019.12.017.

Zhang, L., Xiao, J., Zheng, Y., Li, S., Zhou, Y., 2020. Increased carbon uptake and water use efficiency in global semi-arid ecosystems. Environ. Res. Lett. 15 https://doi.org/10.1088/1748-9326/ab68ec.

Zhang, T., Yang, R., Yang, Y., Li, L., Chen, L., 2021. Assessing the urban eco-environmental quality by the remote-sensing ecological index: application to Tianjin, North China. ISPRS Int. J. Geo-Inform. 10 https://doi.org/10.3390/ijgi10070475.

Zhao, X., Han, D., Lu, Q., Li, Y., Zhang, F., 2023. Spatiotemporal variations in ecological quality of Otindag Sandy land based on a new modified remote sensing ecological index. J. Arid. Land 15, 920–939. https://doi.org/10.1007/s40333-023-0065-9.

Zheng, Z., Wu, Z., Chen, Y., Guo, C., Marinello, F., 2022. Instability of remote sensing based ecological index (RSEI) and its improvement for time series analysis. Sci. Total Environ. 814, 152595 https://doi.org/10.1016/j.scitotenv.2021.152595.

Zhu, J., Zhu, S., Yu, F., Zhang, G., Xu, Y., 2021. A downscaling method for ERA5 reanalysis land surface temperature over urban and mountain areas. Natl. Remote Sens. Bull. 25, 1778–1791. https://doi.org/10.11834/jrs.20211257.